# Performance Analysis of Forward-Backward Matched-Filterbank Spectral Estimators

Hongbin Li, *Student Member, IEEE*, Jian Li, *Senior Member, IEEE*, and Petre Stoica, *Fellow, IEEE*

***Abstract*— The problem of complex spectral estimation is of great interest in many applications. This paper studies the general class of the forward-backward matched-filterbank (MAFI) spectral estimators including the widely used Capon as well as the more recently introduced amplitude and phase estimation of a sinusoid (APES) methods. In particular, we show by means of a higher order expansion technique that the one-dimensional (1-D) Capon estimator underestimates the true spectrum, whereas the 1-D APES method is unbiased; we also show that the bias of the forward-backward Capon is half that of the forward-only Capon (to within a second-order approximation). Furthermore, we show that these results can be extended to the two-dimensional (2-D) Capon and APES estimators. Numerical examples are also presented to demonstrate quantitatively the properties of and the relation between these MAFI estimators.**

## I. Introduction

COMPLEX spectral estimation is important in a variety of applications such as target range signature estimation and synthetic aperture radar (SAR) imaging [1]. Many nonparametric complex spectral estimators make use of adaptive finite impulse response (FIR) filterbanks. An important member of this class of approaches is the Capon spectral estimator [2], [3]. The fact that Capon is actually a *matched-filterbank* (MAFI) spectral estimator was elaborated in [4]. It was found that Capon and the more recently introduced amplitude and phase estimation of a sinusoid (APES) method [1] are both members of the class of the MAFI spectral estimators. A number of results on the statistical and computational performance of the Capon and APES estimators were also presented in [4]. However, the study in [4] was somewhat limited since it only considered *forward-only* MAFI estimators. Owing to the general belief that *forward-backward* approaches usually provide better estimation results and hence are more often used than their forward-only counterparts [5], the more interesting question would be how the forward-backward MAFI estimators perform when compared with one another as well as with their forward-only counterparts.

In this paper, we study the more general forward-backward MAFI estimators. By making use of a higher order expansion technique, we prove that Capon is biased downward, whereas APES is unbiased (to within a second-order approximation). In addition, we find that the bias of the forward-backward Capon is approximately half that of the forward-only Capon. An analysis of the two-dimensional (2-D) extensions of these MAFI estimators reveals that the 2-D MAFI estimators behave similarly to their one-dimensional (1-D) counterparts, which is due to the fact that a *persymmetric* [6] structure of the covariance matrix is retained in the 2-D MAFI estimators. The theoretical results in the paper, supplemented with the empirical observation that Capon usually underestimates the spectrum in samples of practical length while APES is nearly unbiased, are believed to provide a compelling reason for preferring APES over Capon.

The MAFI approach to spectral estimation may also be used to devise new spectral estimators. Even though we show here that a reasonable implementation of a seemingly novel MAFI spectral estimator is reduced back to APES, it remains an open issue whether other interesting MAFI spectral estimators exist.

The paper is organized as follows. In Section II, we discuss the forward-backward MAFI methods. The Capon and APES estimators are shown to be special realizations of the MAFI approach. As seen there, the MAFI interpretation provides insights into the Capon and APES estimators and the relations between them. The statistical and computational analyses of the MAFI estimators are given in Section III. We next describe the 2-D extensions of the forward-backward MAFI approaches in Section IV. Section V contains the numerical examples. Finally, we conclude the paper in Section VI.

## II. Forward-Backward MAFI Methods

Filterbank approaches decompose the observations $\{y(n)\}_{n=0}^{N-1}$ of a stationary signal $y(t)$ as

$$\begin{aligned} y(n) &= \alpha(\omega)e^{j\omega n} + e_\omega(n) \\ n &= 0,1,\ldots,N-1; \quad \omega \in [0,2\pi) \end{aligned} \tag{1}$$

where $\alpha(\omega)$ denotes the complex amplitude of the sinusoidal signal with frequency $\omega$, and $e_\omega(n)$ denotes the noise (or residual) term at frequency $\omega$, which is assumed to be zero mean. The problem of interest is to estimate $\alpha(\omega)$ for any given $\omega$.

Manuscript received June 13, 1997; revised January 29, 1998. This work was supported in part by the Office of Naval Research under Grant N00014-96-0817, the National Science Foundation under Grant MIP-9457388, the Advanced Research Project Agency under Grant MDA-972-93-1-0015, the Swedish Research Council for Engineering Sciences (TFR), the Swedish National Board for Technical Development (NUTEK), and the Senior Individual Grant Program of the Swedish Foundation for Strategic Research. The associate editor coordinating the review of this paper and approving it for publication was Dr. Yingbo Hua.

H. Li and J. Li are with Department of Electrical and Computer Engineering, University of Florida, Gainesville, FL 32611 USA (e-mail: li@saturn.ee.ufl.edu).

P. Stoica is with the Systems and Control Group, Uppsala University, Uppsala, Sweden.

Publisher Item Identifier S 1053-587X(98)04427-4.

Briefly stated, most filterbank spectral approaches address the aforementioned problem by following two main steps: a) pass the data $\{y(n)\}$ through a bandpass filter with varying center frequency $\omega$ and b) obtain the estimates $\hat{\alpha}(\omega)$ for $\omega \in [0, 2\pi)$ of the complex amplitude from the filtered data. The bandpass filter used is usually an $M$-tap FIR filter with its coefficient vector given by

$$\mathbf{h}_\omega = [h_1 \quad h_2 \quad \dots \quad h_M]^T \tag{2}$$

where $(\cdot)^T$ denotes the transpose. (The choice of $M$ is discussed in Section V.) Observe that the notation emphasizes the dependence of the vector in (2) on the center frequency $\omega$. Although rules for choosing $\mathbf{h}_\omega$ vary, a rather general one for the choice of a matched filter is discussed in Section II-B.

### A. Forward-Backward Approaches

Let

$$\bar{\mathbf{y}}(l) = [y(l) \quad y(l+1) \quad \dots \quad y(l+M-1)]^T \qquad l = 0, 1, \dots, L-1 \tag{3}$$

be the overlapping vectors constructed from the data $\{y(n)\}$, where $L = N - M + 1$. In what follows, $\bar{\mathbf{y}}(l)$ is referred to as the *forward data vector*. Let $\bar{\mathbf{e}}_\omega(l), l = 0, 1, \dots, L-1$ be formed from $\{e_\omega(n)\}$ in the same manner as $\bar{\mathbf{y}}(l)$ is from $\{y(n)\}$. Then, the forward vectors can be written as

$$\bar{\mathbf{y}}(l) = [\alpha(\omega)\mathbf{a}_M(\omega)]e^{j\omega l} + \bar{\mathbf{e}}_\omega(l) \tag{4}$$

where $\mathbf{a}_M(\omega)$ is given by

$$\mathbf{a}_M(\omega) = [1 \quad e^{j\omega} \quad \dots \quad e^{j(M-1)\omega}]^T. \tag{5}$$

Likewise, the *backward data vectors* are constructed as

$$\tilde{\mathbf{y}}(l) = [y^*(N-l-1) \quad y^*(N-l-2) \quad \dots \quad y^*(N-l-M)]^T, \quad l = 0, 1, \dots, L-1 \tag{6}$$

where $(\cdot)^*$ denotes the complex conjugate. Let $\tilde{\mathbf{e}}_\omega(l), l = 0, 1, \dots, L-1$ be formed from $\{e_\omega(n)\}$ the same way as $\tilde{\mathbf{y}}(l)$ is formed from $\{y(n)\}$. Then, the backward vector can be written as

$$\tilde{\mathbf{y}}(l) = [\tilde{\alpha}(\omega)\mathbf{a}_M(\omega)]e^{j\omega l} + \tilde{\mathbf{e}}_\omega(l) \tag{7}$$

where

$$\tilde{\alpha}(\omega) = \alpha^*(\omega)e^{-j(N-1)\omega}. \tag{8}$$

It is straightforward to verify that the forward and backward vectors are related by the complex conjugate symmetry property

$$\tilde{\mathbf{y}}(l) = \mathbf{J}\bar{\mathbf{y}}^*(L-l-1) \tag{9}$$

where $\mathbf{J}$ denotes the exchange matrix whose antidiagonal elements are ones and all the others are zero.

Suppose that the initial phase of the sinusoidal signal in (1) is a random variable uniformly distributed over the interval $[0, 2\pi)$ and independent of the noise term. By making use of this assumption as well as (9), the covariance matrix of $\bar{\mathbf{y}}(l)$ or, equivalently, of $\tilde{\mathbf{y}}(l)$, is given by

$$\begin{aligned}\mathbf{R} &\triangleq E\{\bar{\mathbf{y}}(l)\bar{\mathbf{y}}^H(l)\} = E\{\tilde{\mathbf{y}}(l)\tilde{\mathbf{y}}^H(l)\} \\ &= |\alpha(\omega)|^2\mathbf{a}_M(\omega)\mathbf{a}_M^H(\omega) + \mathbf{Q}(\omega)\end{aligned} \tag{10}$$

where $(\cdot)^H$ denotes the conjugate transpose, and $\mathbf{Q}(\omega)$ is the noise covariance matrix and is given by

$$\mathbf{Q}(\omega) \triangleq E\{\bar{\mathbf{e}}_\omega(l)\bar{\mathbf{e}}_\omega^H(l)\} = E\{\tilde{\mathbf{e}}_\omega(l)\tilde{\mathbf{e}}_\omega^H(l)\}. \tag{11}$$

Note that both $\mathbf{R}$ and $\mathbf{Q}$ are Hermitian Toeplitz matrices. Let $\hat{\bar{\mathbf{R}}}$ and $\hat{\tilde{\mathbf{R}}}$, respectively, denote the sample covariance matrices of $\{\bar{\mathbf{y}}(l)\}$ and $\{\tilde{\mathbf{y}}(l)\}$, that is

$$\hat{\bar{\mathbf{R}}} = \frac{1}{L}\sum_{l=0}^{L-1}\bar{\mathbf{y}}(l)\bar{\mathbf{y}}^H(l) \tag{12}$$

$$\hat{\tilde{\mathbf{R}}} = \frac{1}{L}\sum_{l=0}^{L-1}\tilde{\mathbf{y}}(l)\tilde{\mathbf{y}}^H(l). \tag{13}$$

(Note that since $\hat{\tilde{\mathbf{R}}} = \mathbf{J}\hat{\bar{\mathbf{R}}}^T\mathbf{J}$, which follows from (9), there is no need to compute $\hat{\tilde{\mathbf{R}}}$ separately.) The forward-backward estimate of $\mathbf{R}$ is given by

$$\hat{\mathbf{R}} = \frac{1}{2}(\hat{\bar{\mathbf{R}}} + \hat{\tilde{\mathbf{R}}}). \tag{14}$$

The $\hat{\mathbf{R}}$ in (14) is Hermitian but no longer Toeplitz. By using (9), we can show that $\hat{\mathbf{R}}$ is a *persymmetric* matrix [6], i.e.,

$$\hat{\mathbf{R}} = \mathbf{J}\hat{\mathbf{R}}^T\mathbf{J}. \tag{15}$$

The forward-backward approaches use both the forward and backward data vectors to obtain the estimate $\hat{\mathbf{R}}$ of $\mathbf{R}$, whereas the forward-only approaches use only the forward data vectors to estimate $\mathbf{R}$ by $\hat{\bar{\mathbf{R}}}$. As $\mathbf{R}$ is persymmetric, we can expect that $\hat{\mathbf{R}}$ is generally a better estimate of $\mathbf{R}$ than $\hat{\bar{\mathbf{R}}}$.

### B. MAFI Filters

By definition, the matched filter is designed such that the corresponding signal-to-noise (SNR) ratio in the filter output is maximized, that is

$$\mathbf{h}_\omega = \arg\max_{\mathbf{h}_\omega} \frac{\left|\mathbf{h}_\omega^H\mathbf{a}_M(\omega)\right|^2}{\mathbf{h}_\omega^H\mathbf{Q}(\omega)\mathbf{h}_\omega}. \tag{16}$$

The solution is obtained by making use of the Cauchy–Schwartz inequality (see, e.g., [7])

$$\mathbf{h}_\omega = \frac{\mathbf{Q}^{-1}(\omega)\mathbf{a}_M(\omega)}{\mathbf{a}_M^H(\omega)\mathbf{Q}^{-1}(\omega)\mathbf{a}_M(\omega)} \tag{17}$$

where $\mathbf{Q}(\omega)$ is assumed to be invertible. It is readily checked that the solution in (17) satisfies

$$\mathbf{h}_\omega^H\mathbf{a}_M(\omega) = 1 \tag{18}$$

which implies that the filter given in (17) passes the frequency $\omega$ undistorted. This property is a basic requirement of all

filterbank approaches. By making use of this observation and of (4) and (7), we have

$$\mathbf{h}_\omega^H \bar{\mathbf{y}}(l) = \alpha(\omega)e^{j\omega l} + \mathbf{h}_\omega^H \bar{\mathbf{e}}_\omega(l), \quad l = 0, 1, \ldots, L-1 \quad (19)$$

and

$$\mathbf{h}_\omega^H \tilde{\mathbf{y}}(l) = e^{-j(N-1)\omega}\alpha^*(\omega)e^{j\omega l} + \mathbf{h}_\omega^H \tilde{\mathbf{e}}_\omega(l) \quad l = 0, 1, \ldots, L-1. \quad (20)$$

The least squares (LS) estimate of $\alpha(\omega)$ obtained by using (19) and (20) is given by

$$\hat{\alpha}(\omega) = \frac{1}{2}\left[\mathbf{h}_\omega^H \bar{\mathbf{g}}(\omega) + e^{-j(N-1)\omega}\tilde{\mathbf{g}}^H(\omega)\mathbf{h}_\omega\right] \quad (21)$$

where $\bar{\mathbf{g}}(\omega)$ and $\tilde{\mathbf{g}}(\omega)$ are, respectively, the normalized Fourier transforms of the forward and backward data vectors

$$\bar{\mathbf{g}}(\omega) = \frac{1}{L}\sum_{l=0}^{L-1} \bar{\mathbf{y}}(l)e^{-j\omega l} \quad (22)$$

$$\tilde{\mathbf{g}}(\omega) = \frac{1}{L}\sum_{l=0}^{L-1} \tilde{\mathbf{y}}(l)e^{-j\omega l}. \quad (23)$$

Since $\mathbf{Q}(\omega)$ is Toeplitz and, therefore, persymmetric, we can show that the $\mathbf{h}_\omega$ in (17) satisfies [1]

$$\mathbf{J}\mathbf{h}_\omega^* = \mathbf{h}_\omega e^{-j(M-1)\omega}. \quad (24)$$

Consequently, it follows, after some calculation, that (21) is equivalent to

$$\hat{\alpha}(\omega) = \mathbf{h}_\omega^H \bar{\mathbf{g}}(\omega). \quad (25)$$

Hence, due to the persymmetry of $\mathbf{Q}(\omega)$, the forward-backward estimate of $\alpha(\omega)$ has the same form as the forward-only estimate of $\alpha(\omega)$, i.e., both are given by (25). However, the filter vector $\mathbf{h}_\omega$ obtained with the forward-backward approach is different from that corresponding to the forward-only approach [1].

Although neither Capon nor APES was derived in the MAFI framework (for original derivations of these methods, we refer to [1], [2], and [7]), in what follows, we show that two natural estimators of $\mathbf{Q}(\omega)$ in (17) lead to the Capon and APES filters, respectively. More interestingly, we also show that even though a third natural estimator of $\mathbf{Q}(\omega)$ gives a new filter that is different from the former two, the spectral estimator corresponding to the new filter turns out to be equivalent to APES as well.

*Capon Filter:* By (10), one natural choice is to estimate $\mathbf{Q}(\omega)$ as

$$\hat{\mathbf{Q}}(\omega) = \hat{\mathbf{R}} - |\hat{\alpha}(\omega)|^2 \mathbf{a}_M(\omega)\mathbf{a}_M^H(\omega) \quad (26)$$

where $\hat{\alpha}(\omega)$ is some estimate of $\alpha(\omega)$, and $\hat{\mathbf{R}}$ is the forward-backward sample covariance matrix given in (14). By making use of the matrix inversion lemma [6], we can see that the second term in (26) has no influence on the $\mathbf{h}_\omega$ in (17). Hence, when (26) is substituted into (17), the matched filter reduces to the Capon filter [2], [3]

$$\mathbf{h}_\omega^{\text{Capon}} = \frac{\hat{\mathbf{R}}^{-1}\mathbf{a}_M(\omega)}{\mathbf{a}_M^H(\omega)\hat{\mathbf{R}}^{-1}\mathbf{a}_M(\omega)}. \quad (27)$$

Since $\hat{\mathbf{Q}}(\omega)$ is persymmetric, (25) applies. By substituting (27) into (25), we obtain the Capon estimate of $\alpha(\omega)$

$$\hat{\alpha}_{\text{Capon}}(\omega) = \frac{\mathbf{a}_M^H(\omega)\hat{\mathbf{R}}^{-1}\bar{\mathbf{g}}(\omega)}{\mathbf{a}_M^H(\omega)\hat{\mathbf{R}}^{-1}\mathbf{a}_M(\omega)}. \quad (28)$$

The forward-only Capon estimate of $\alpha(\omega)$ has a similar form, except that $\hat{\mathbf{R}}$ is replaced by $\hat{\bar{\mathbf{R}}}$.

*APES Filter:* Ignoring the fact that $\mathbf{a}_M(\omega)$ is known, we obtain the LS estimate of the vector $\alpha(\omega)\mathbf{a}_M(\omega)$ in (4) as

$$\widehat{[\alpha(\omega)\mathbf{a}_M(\omega)]} = \bar{\mathbf{g}}(\omega). \quad (29)$$

Inserting (29) into (26) will yield a plausible estimate of $\mathbf{Q}(\omega)$. Yet, the so-obtained $\hat{\mathbf{Q}}(\omega)$ is not persymmetric. Observe that an estimate of $\mathbf{Q}(\omega)$ that uses only the forward data vectors can be obtained as

$$\hat{\bar{\mathbf{Q}}}(\omega) = \hat{\bar{\mathbf{R}}} - \widehat{[\alpha(\omega)\mathbf{a}_M(\omega)]}\widehat{[\alpha(\omega)\mathbf{a}_M(\omega)]}^H = \hat{\bar{\mathbf{R}}} - \bar{\mathbf{g}}(\omega)\bar{\mathbf{g}}^H(\omega). \quad (30)$$

A persymmetric estimate of $\mathbf{Q}(\omega)$ can be obtained by using both the forward and backward data vectors

$$\hat{\mathbf{Q}}(\omega) = \frac{1}{2}\left[\hat{\bar{\mathbf{Q}}}(\omega) + \mathbf{J}\hat{\bar{\mathbf{Q}}}^T(\omega)\mathbf{J}\right] = \hat{\mathbf{R}} - \mathbf{G}(\omega)\mathbf{G}^H(\omega) \quad (31)$$

where

$$\mathbf{G}(\omega) = \frac{1}{\sqrt{2}}[\bar{\mathbf{g}}(\omega) \quad \tilde{\mathbf{g}}(\omega)] \quad (32)$$

and we have used the fact that $\mathbf{J}\bar{\mathbf{g}}^*(\omega) = e^{j\omega(L-1)}\tilde{\mathbf{g}}(\omega)$. Using this $\hat{\mathbf{Q}}(\omega)$ in (17) yields the APES filter [1]

$$\mathbf{h}_\omega^{\text{APES}} = \frac{\hat{\mathbf{Q}}^{-1}(\omega)\mathbf{a}_M(\omega)}{\mathbf{a}_M^H(\omega)\hat{\mathbf{Q}}^{-1}(\omega)\mathbf{a}_M(\omega)}. \quad (33)$$

Consequently, the APES estimate of $\alpha(\omega)$ is given by [see (25)]

$$\hat{\alpha}_{\text{APES}}(\omega) = \frac{\mathbf{a}_M^H(\omega)\hat{\mathbf{Q}}^{-1}(\omega)\bar{\mathbf{g}}(\omega)}{\mathbf{a}_M^H(\omega)\hat{\mathbf{Q}}^{-1}(\omega)\mathbf{a}_M(\omega)}. \quad (34)$$

Like the Capon estimates, the forward-only APES estimate of $\alpha(\omega)$ is similar to (34), except that $\hat{\mathbf{Q}}(\omega)$ is replaced by $\hat{\bar{\mathbf{Q}}}(\omega)$ [1].

*Another Matched Filter:* Equations (4) and (7) suggest another way to estimate the noise covariance matrix $\mathbf{Q}(\omega)$

$$\begin{aligned}\hat{\mathbf{Q}}(\omega) &= \frac{1}{2L}\sum_{l=0}^{L-1}[(\bar{\mathbf{y}}(l) - \hat{\alpha}(\omega)\mathbf{a}_M(\omega)e^{j\omega l}) \\ &\times (\bar{\mathbf{y}}(l) - \hat{\alpha}(\omega)\mathbf{a}_M(\omega)e^{j\omega l})^H + (\tilde{\mathbf{y}}(l) - \hat{\tilde{\alpha}}(\omega)\mathbf{a}_M(\omega)e^{j\omega l}) \\ &\times (\tilde{\mathbf{y}}(l) - \hat{\tilde{\alpha}}(\omega)\mathbf{a}_M(\omega)e^{j\omega l})^H] \end{aligned} \quad (35)$$

where $\hat{\alpha}(\omega)$ and $\hat{\tilde{\alpha}}(\omega) = \hat{\alpha}^*(\omega)e^{-j(N-1)\omega}$ denote some estimates of $\alpha(\omega)$ and $\tilde{\alpha}(\omega)$, respectively. A simple calculation shows that the previous $\hat{\mathbf{Q}}(\omega)$ can be rewritten as (in

what follows, we sometimes omit the dependence on $\omega$ for notational convenience)

$$\hat{\mathbf{Q}}(\omega) = \underbrace{\hat{\mathbf{R}} - \frac{1}{2}[\hat{\alpha}^*\bar{\mathbf{g}} + \hat{\bar{\alpha}}^*\tilde{\mathbf{g}}]\mathbf{a}_M^H}_{\mathbf{\Omega}} - \frac{1}{2}\mathbf{a}_M[\hat{\alpha}^*\bar{\mathbf{g}} + \hat{\bar{\alpha}}^*\tilde{\mathbf{g}}]^H + |\hat{\alpha}|^2\mathbf{a}_M\mathbf{a}_M^H. \tag{36}$$

By using the matrix inversion lemma (twice), we can see that the last and the third terms of (36) can be dropped without affecting the matched filter vector. Let $\mathbf{\Omega}$ be the matrix made from the first two terms of (36). Then, by using the matrix inversion lemma once again, we have (37), shown at the bottom of the page, which gives, for the matched filter vector, (38), also shown at the bottom of the page. The previous filter is, in general, different from both the Capon and APES filters since neither of the latter two depends on an estimate of $\alpha(\omega)$, whereas the former does. In spite of this fact, in Appendix A, we prove that, for a certain natural choice of $\hat{\alpha}(\omega)$ in (35)

$$\hat{\alpha}_{\mathrm{MAFI}}(\omega) = \hat{\alpha}_{\mathrm{APES}}(\omega) \tag{39}$$

holds true.

## III. Computational and Statistical Analysis

### A. Computational Complexity

Applying the matrix inversion lemma to (31) yields

$$\hat{\mathbf{Q}}^{-1}(\omega) = \hat{\mathbf{R}}^{-1} - \hat{\mathbf{R}}^{-1}\mathbf{G}(\omega)[\mathbf{G}^H(\omega)\hat{\mathbf{R}}^{-1}\mathbf{G}(\omega) - \mathbf{I}]^{-1} \times \mathbf{G}^H(\omega)\hat{\mathbf{R}}^{-1} \tag{40}$$

where $\mathbf{I}$ is the $2 \times 2$ identity matrix. Let $\hat{\mathbf{R}}^{-1/2}$ denote the Hermitian square root of the positive definite matrix $\hat{\mathbf{R}}^{-1}$. Let

$$\boldsymbol{\nu}_1(\omega) = \hat{\mathbf{R}}^{-1/2}\mathbf{a}_M(\omega) \tag{41}$$

$$\boldsymbol{\nu}_2(\omega) = \hat{\mathbf{R}}^{-1/2}\bar{\mathbf{g}}(\omega) \tag{42}$$

$$\boldsymbol{\nu}_3(\omega) = \hat{\mathbf{R}}^{-1/2}\tilde{\mathbf{g}}(\omega). \tag{43}$$

The Capon and APES spectral estimators can be expressed as relatively simple functions of $\boldsymbol{\nu}_i(\omega), i = 1, 2, 3$

$$\hat{\alpha}_{\mathrm{Capon}}(\omega) = \frac{\boldsymbol{\nu}_1^H(\omega)\boldsymbol{\nu}_2(\omega)}{\|\boldsymbol{\nu}_1(\omega)\|^2} \tag{44}$$

and (45), shown at the bottom of the page, where

$$\mathbf{\Xi}(\omega) = \frac{1}{2}\begin{bmatrix} \|\boldsymbol{\nu}_2(\omega)\|^2 & \boldsymbol{\nu}_2^H(\omega)\boldsymbol{\nu}_3(\omega) \\ \boldsymbol{\nu}_3^H(\omega)\boldsymbol{\nu}_2(\omega) & \|\boldsymbol{\nu}_3(\omega)\|^2 \end{bmatrix} - \mathbf{I}. \tag{46}$$

Hence, computationally, APES is only slightly more involved than Capon. More specifically, the amount of computation required by Capon or APES is dominated by calculating $\hat{\mathbf{R}}^{-1/2}$ and the matrix-vector products in (41)–(43). By using (83), as well as the facts that $\|\boldsymbol{\nu}_2\|^2 = \|\boldsymbol{\nu}_3\|^2$ and $\left(\boldsymbol{\nu}_1^H\boldsymbol{\nu}_2\right)^* e^{-j(N-1)\omega} = \boldsymbol{\nu}_1^H\boldsymbol{\nu}_3$, which follow from (9), it is clear that the additional amount of computation needed by APES, as compared with Capon, is fairly small (see Section V for the simulation results). Note that using (44) and (45) for the implementation of Capon and APES requires calculating (41)–(43) for each $\omega$ of interest, which becomes computationally increasingly more intensive as the number of frequency samples increases. This is especially so in 2-D applications, such as when forming SAR images. By using a technique recently presented in [8], however, the amount of computation by both Capon and APES can be substantially reduced. Refer to [8] for more implementation details. Nevertheless, it is convenient to use (44) and (45) to visually compare the computational complexities of Capon and APES.

$$\mathbf{\Omega}^{-1}\mathbf{a}_M = \left[\hat{\mathbf{R}} - \frac{1}{2}(\hat{\alpha}^*\bar{\mathbf{g}} + \hat{\bar{\alpha}}^*\tilde{\mathbf{g}})\mathbf{a}_M^H\right]^{-1}\mathbf{a}_M = \left[\hat{\mathbf{R}}^{-1} + \frac{\frac{1}{2}\hat{\mathbf{R}}^{-1}(\hat{\alpha}^*\bar{\mathbf{g}} + \hat{\bar{\alpha}}^*\tilde{\mathbf{g}})\mathbf{a}_M^H\hat{\mathbf{R}}^{-1}}{1 - \frac{1}{2}\mathbf{a}_M^H\hat{\mathbf{R}}^{-1}(\hat{\alpha}^*\bar{\mathbf{g}} + \hat{\bar{\alpha}}^*\tilde{\mathbf{g}})}\right]\mathbf{a}_M = \frac{\hat{\mathbf{R}}^{-1}\mathbf{a}_M - \frac{1}{2}\mathbf{a}_M^H\hat{\mathbf{R}}^{-1}[\hat{\alpha}^*\bar{\mathbf{g}} + \hat{\bar{\alpha}}^*\tilde{\mathbf{g}}]\hat{\mathbf{R}}^{-1}\mathbf{a}_M + \frac{1}{2}\mathbf{a}_M^H\hat{\mathbf{R}}^{-1}\mathbf{a}_M\hat{\mathbf{R}}^{-1}[\hat{\alpha}^*\bar{\mathbf{g}} + \hat{\bar{\alpha}}^*\tilde{\mathbf{g}}]}{1 - \frac{1}{2}\mathbf{a}_M^H\hat{\mathbf{R}}^{-1}[\hat{\alpha}^*\bar{\mathbf{g}} + \hat{\bar{\alpha}}^*\tilde{\mathbf{g}}]} \tag{37}$$

$$\mathbf{h}_\omega^{\mathrm{MAFI}} = \frac{\mathbf{\Omega}^{-1}\mathbf{a}_M}{\mathbf{a}_M^H\mathbf{\Omega}^{-1}\mathbf{a}_M} = \frac{\hat{\mathbf{R}}^{-1}\mathbf{a}_M + \frac{1}{2}\mathbf{a}_M^H\hat{\mathbf{R}}^{-1}\mathbf{a}_M\hat{\mathbf{R}}^{-1}[\hat{\alpha}^*\bar{\mathbf{g}} + \hat{\bar{\alpha}}^*\tilde{\mathbf{g}}] - \frac{1}{2}\mathbf{a}_M^H\hat{\mathbf{R}}^{-1}[\hat{\alpha}^*\bar{\mathbf{g}} + \hat{\bar{\alpha}}^*\tilde{\mathbf{g}}]\hat{\mathbf{R}}^{-1}\mathbf{a}_M}{\mathbf{a}_M^H\hat{\mathbf{R}}^{-1}\mathbf{a}_M}. \tag{38}$$

$$\hat{\alpha}_{\mathrm{APES}}(\omega) = \frac{\boldsymbol{\nu}_1^H(\omega)\boldsymbol{\nu}_2(\omega) - \frac{1}{2}\begin{bmatrix}\boldsymbol{\nu}_1^H(\omega)\boldsymbol{\nu}_2(\omega) & \boldsymbol{\nu}_1^H(\omega)\boldsymbol{\nu}_3(\omega)\end{bmatrix}\mathbf{\Xi}^{-1}(\omega)\begin{bmatrix}\|\boldsymbol{\nu}_2(\omega)\|^2 \\ \boldsymbol{\nu}_3^H(\omega)\boldsymbol{\nu}_2(\omega)\end{bmatrix}}{\|\boldsymbol{\nu}_1(\omega)\|^2 - \frac{1}{2}\begin{bmatrix}\boldsymbol{\nu}_1^H(\omega)\boldsymbol{\nu}_2(\omega) & \boldsymbol{\nu}_1^H(\omega)\boldsymbol{\nu}_3(\omega)\end{bmatrix}\mathbf{\Xi}^{-1}(\omega)\begin{bmatrix}\boldsymbol{\nu}_2^H(\omega)\boldsymbol{\nu}_1(\omega) \\ \boldsymbol{\nu}_3^H(\omega)\boldsymbol{\nu}_1(\omega)\end{bmatrix}} \tag{45}$$

### B. Statistical Performance

The forward-backward Capon and APES spectral estimators can be shown to have the same *asymptotic variance* under the following condition:

**C:** The signal $y(n)$ can be written as in (1), where $e_\omega(n)$ is a zero-mean stationary random process with finite spectral density at $\omega$

$$P_e(\omega) < \infty. \tag{47}$$

In more exact terms, the following result holds true.

*Theorem 1:* Under Condition **C** and the additional assumption that $e_\omega(n)$ is circularly symmetrically distributed, the estimation errors in the Capon and APES spectral estimators are asymptotically circularly symmetrically distributed with zero-mean and the common variance

$$\lim_{L\to\infty} LE\{|\hat{\alpha}(\omega) - \alpha(\omega)|^2\} = P_e(\omega). \tag{48}$$

*Proof:* See Appendix B. □

The need to enforce Condition **C** limits, to some extent, the importance of the previous result. Indeed, the assumption made in **C** is satisfied if (and essentially only if) the signal $y(n)$ has a mixed spectrum, *and* $\omega$ is the location of a spectral line. The result of Theorem 1 is relevant to the spectral analysis of a target with dominant point scatterers in the presence of distributed clutter (see [1] and the references therein). In some other applications, however, the main interest is in the continuous component of the spectrum. For example, Condition **C** does not hold exactly for a target with distributed scatterers since the signature spectrum is continuous at $\omega$.

That the previous result is of a somewhat limited interest is also due to its *asymptotic character*. Indeed, in applications with medium or small-sized data samples, the spectral estimators under study have been found to behave quite differently in contradiction with what is predicted by the (asymptotic) result of Theorem 1 (see the numerical examples in Section V). The *finite-sample analysis* of the spectral estimators under discussion would consequently be of considerable interest. However, a complete analysis, if possible, appears to be rather difficult at best. A *partial* one, by making use of a *higher-order Taylor expansion technique*, is nevertheless feasible. The result follows.

*Theorem 2:* To within a second-order approximation and under the mild assumption that the third-order moments of $\bar{\mathbf{e}}_\omega(n)$ and $\tilde{\mathbf{e}}_\omega(n)$ are zero, Capon is biased downward, whereas APES is unbiased, that is

$$\frac{LE\{\hat{\alpha}_{\text{Capon}}(\omega) - \alpha(\omega)\}}{\alpha(\omega)} < 0 \tag{49}$$

and

$$LE\{\hat{\alpha}_{\text{APES}}(\omega) - \alpha(\omega)\} = 0 \tag{50}$$

for sufficiently large values of $L$. Additionally, the bias for the forward-backward Capon is half that of the forward-only Capon.

*Proof:* See Appendix C. □

We believe that (49) and (50) provide a theoretical motivation for preferring APES to Capon in most spectral estimation exercises. Moreover, Theorem 2 also suggests that the forward-backward Capon should be preferred over the forward-only Capon. While the forward-only APES is also unbiased [4], the forward-backward APES is usually observed with slightly better resolution and sidelobe properties [1] at the cost of slightly more computations.

## IV. 2-D Extensions

We briefly describe the 2-D extensions of the forward-backward MAFI spectral estimators. We first decompose the observations $\{y(n_1,n_2)\}$ as

$$\begin{aligned} y(n_1,n_2) &= \alpha(\omega_1,\omega_2)e^{j(\omega_1 n_1+\omega_2 n_2)} + e_{\omega_1,\omega_2}(n_1,n_2) \\ & n_1 = 0,1,\ldots,N_1-1; \quad n_2 = 0,1,\ldots,N_2-1 \\ & \omega_1,\omega_2 \in [0,2\pi) \end{aligned} \tag{51}$$

where $\alpha(\omega_1,\omega_2)$ denotes the complex amplitude of a 2-D sinusoidal signal with frequency $(\omega_1,\omega_2)$, and $e_{\omega_1,\omega_2}(n_1,n_2)$ denotes the noise (or residual) term at frequency $(\omega_1,\omega_2)$, which is assumed to be zero mean. Next, in a manner similar to the 1-D case, we form the $M_1\times M_2$ *forward and backward data matrices*

$$\begin{aligned} \bar{\mathbf{Y}}(l_1,l_2) &= \{y(n_1,n_2), \quad n_1 = l_1,\ldots,l_1+M_1-1 \\ &\qquad n_2 = l_2,\ldots,l_2+M_2-1\} \\ \tilde{\mathbf{Y}}(l_1,l_2) &= \{y^*(n_1,n_2) \\ &\qquad n_1 = N_1-l_1-1,\ldots,N_1-l_1-M_1 \\ &\qquad n_2 = N_2-l_2-1,\ldots,N_2-l_2-M_2\} \\ & l_1 = 0,1,\ldots,L_1-1; \quad l_2 = 0,1,\ldots,L_2-1 \end{aligned} \tag{52}$$

where $L_1 = N_1 - M_1 + 1$ and $L_2 = N_2 - M_2 + 1$. Let

$$\bar{\mathbf{y}}(l_1,l_2) = \text{vec}[\bar{\mathbf{Y}}(l_1,l_2)] \tag{53}$$

$$\tilde{\mathbf{y}}(l_1,l_2) = \text{vec}[\tilde{\mathbf{Y}}(l_1,l_2)] \tag{54}$$

where vec$[\cdot]$ denotes the operation of stacking the columns of a matrix on top of each other. Let

$$\mathbf{a}_{M_1,M_2}(\omega_1,\omega_2) = \mathbf{a}_{M_2}(\omega_2)\otimes\mathbf{a}_{M_1}(\omega_1) \tag{55}$$

where $\otimes$ denotes the Kronecker matrix product, and

$$\mathbf{a}_{M_k}(\omega_k) = [1 \quad e^{j\omega_k} \quad \ldots \quad e^{j(M_k-1)\omega_k}]^T, \quad k = 1,2. \tag{56}$$

Then, $\bar{\mathbf{y}}(l_1,l_2)$ and $\tilde{\mathbf{y}}(l_1,l_2)$ can be written as

$$\begin{aligned} \bar{\mathbf{y}}(l_1,l_2) &= \left[\alpha(\omega_1,\omega_2)\mathbf{a}_{M_1,M_2}(\omega_1,\omega_2)\right]e^{j(\omega_1 l_1+\omega_2 l_2)} \\ &\quad + \bar{\mathbf{e}}_{\omega_1,\omega_2}(l_1,l_2) \end{aligned} \tag{57}$$

$$\begin{aligned} \tilde{\mathbf{y}}(l_1,l_2) &= \left[\tilde{\alpha}(\omega_1,\omega_2)\mathbf{a}_{M_1,M_2}(\omega_1,\omega_2)\right]e^{j(\omega_1 l_1+\omega_2 l_2)} \\ &\quad + \tilde{\mathbf{e}}_{\omega_1,\omega_2}(l_1,l_2) \end{aligned} \tag{58}$$

where

$$\tilde{\alpha}(\omega_1,\omega_2) = \alpha^*(\omega_1,\omega_2)e^{-j(N_1-1)\omega_1}e^{-j(N_2-1)\omega_2} \tag{59}$$

and $\bar{\mathbf{e}}_{\omega_1,\omega_2}(l_1,l_2)$ and $\tilde{\mathbf{e}}_{\omega_1,\omega_2}(l_1,l_2)$ are, respectively, formed from $\{e_{\omega_1,\omega_2}(n_1,n_2)\}$ in the same ways as $\bar{\mathbf{y}}(l_1,l_2)$ and $\tilde{\mathbf{y}}(l_1,l_2)$ are made from $\{y(n_1,n_2)\}$.

Suppose that the initial phase of the sinusoidal signal of (51) is a random variable uniformly distributed over the interval $[0, 2\pi)$ and independent of the noise term. Then, the covariance matrix of $\bar{\mathbf{y}}(l_1, l_2)$ or, equivalently, of $\tilde{\mathbf{y}}(l_1, l_2)$ is given by

$$\mathbf{R} = |\alpha(\omega_1, \omega_2)|^2 \mathbf{a}_{M_1,M_2}(\omega_1, \omega_2)\mathbf{a}^H_{M_1,M_2}(\omega_1, \omega_2) + \mathbf{Q}(\omega_1, \omega_2) \tag{60}$$

where $\mathbf{Q}(\omega_1, \omega_2)$ is the covariance matrix of $\bar{\mathbf{e}}_{\omega_1,\omega_2}(l_1, l_2)$ or $\tilde{\mathbf{e}}_{\omega_1,\omega_2}(l_1, l_2)$. By making use of the fact that

$$\tilde{\mathbf{y}}(l_1, l_2) = \mathbf{J}\bar{\mathbf{y}}^*(L_1 - l_1 - 1, L_2 - l_2 - 1) \tag{61}$$

we can see that $\mathbf{R}$ is persymmetric. Similarly, $\mathbf{Q}$ is also persymmetric.

The forward-backward sample covariance matrix takes the form

$$\hat{\mathbf{R}} = \frac{1}{2}(\hat{\bar{\mathbf{R}}} + \hat{\tilde{\mathbf{R}}}) \tag{62}$$

where $\hat{\bar{\mathbf{R}}}$ and $\hat{\tilde{\mathbf{R}}}$ denote the sample covariance matrices of $\{\bar{\mathbf{y}}(l_1, l_2)\}$ and $\{\tilde{\mathbf{y}}(l_1, l_2)\}$, respectively, given by

$$\hat{\bar{\mathbf{R}}} = \frac{1}{L_1 L_2} \sum_{l_1=0}^{L_1-1} \sum_{l_2=0}^{L_2-1} \bar{\mathbf{y}}(l_1, l_2)\bar{\mathbf{y}}^H(l_1, l_2) \tag{63}$$

$$\hat{\tilde{\mathbf{R}}} = \frac{1}{L_1 L_2} \sum_{l_1=0}^{L_1-1} \sum_{l_2=0}^{L_2-1} \tilde{\mathbf{y}}(l_1, l_2)\tilde{\mathbf{y}}^H(l_1, l_2). \tag{64}$$

By making use of (61), we can see that $\hat{\mathbf{R}}$ is also persymmetric.

Let $\mathbf{H}_{\omega_1,\omega_2}$ denote the impulse response of an $M_1 \times M_2$ 2-D FIR filter, and let

$$\mathbf{h}_{\omega_1,\omega_2} = \mathrm{vec}\big[\mathbf{H}_{\omega_1,\omega_2}\big]. \tag{65}$$

Like in the 1-D case, the impulse response of the matched filter is given by

$$\mathbf{h}_{\omega_1,\omega_2} = \frac{\mathbf{Q}^{-1}(\omega_1, \omega_2)\mathbf{a}_{M_1,M_2}(\omega_1, \omega_2)}{\mathbf{a}^H_{M_1,M_2}(\omega_1, \omega_2)\mathbf{Q}^{-1}(\omega_1, \omega_2)\mathbf{a}_{M_1,M_2}(\omega_1, \omega_2)}. \tag{66}$$

Since

$$\mathbf{h}^H_{\omega_1,\omega_2}\mathbf{a}_{M_1,M_2}(\omega_1, \omega_2) = 1 \tag{67}$$

the LS estimate of $\alpha$ obtained from the filtered data is given by [similarly to (21) in the 1-D case]

$$\hat{\alpha}(\omega_1, \omega_2) = \frac{1}{2}\big[\mathbf{h}^H_{\omega_1,\omega_2}\bar{\mathbf{g}}(\omega_1, \omega_2) + e^{-j(N_1-1)\omega_1} \times e^{-j(N_2-1)\omega_2}\tilde{\mathbf{g}}^H(\omega_1, \omega_2)\mathbf{h}_{\omega_1,\omega_2}\big] \tag{68}$$

where

$$\bar{\mathbf{g}}(\omega_1, \omega_2) = \frac{1}{L_1 L_2} \sum_{l_1=0}^{L_1-1} \sum_{l_2=0}^{L_2-1} \bar{\mathbf{y}}(l_1, l_2)e^{-j(\omega_1 l_1 + \omega_2 l_2)} \tag{69}$$

$$\tilde{\mathbf{g}}(\omega_1, \omega_2) = \frac{1}{L_1 L_2} \sum_{l_1=0}^{L_1-1} \sum_{l_2=0}^{L_2-1} \tilde{\mathbf{y}}(l_1, l_2)e^{-j(\omega_1 l_1 + \omega_2 l_2)}. \tag{70}$$

Since $\mathbf{Q}$ is persymmetric, (68) can be written as

$$\hat{\alpha}(\omega_1, \omega_2) = \mathbf{h}^H_{\omega_1,\omega_2}\bar{\mathbf{g}}(\omega_1, \omega_2). \tag{71}$$

The Capon method estimates the noise covariance matrix as

$$\hat{\mathbf{Q}}(\omega_1, \omega_2) = \hat{\mathbf{R}} - |\hat{\alpha}(\omega_1, \omega_2)|^2 \mathbf{a}_{M_1,M_2}(\omega_1, \omega_2)\mathbf{a}^H_{M_1,M_2}(\omega_1, \omega_2) \tag{72}$$

where $\hat{\alpha}(\omega_1, \omega_2)$ denotes some estimate of $\alpha(\omega_1, \omega_2)$. The $\mathbf{Q}(\omega_1, \omega_2)$ in (72) can be shown to be persymmetric. Therefore, with (72) substituted in (66) and then (66) substituted in (71), we obtain the Capon estimate of $\alpha(\omega_1, \omega_2)$ as

$$\hat{\alpha}_{\mathrm{Capon}}(\omega_1, \omega_2) = \frac{\mathbf{a}^H_{M_1,M_2}(\omega_1, \omega_2)\hat{\mathbf{R}}^{-1}\bar{\mathbf{g}}(\omega_1, \omega_2)}{\mathbf{a}^H_{M_1,M_2}(\omega_1, \omega_2)\hat{\mathbf{R}}^{-1}\mathbf{a}_{M_1,M_2}(\omega_1, \omega_2)}. \tag{73}$$

The APES estimate of $\mathbf{Q}(\omega_1, \omega_2)$ takes the form

$$\hat{\mathbf{Q}}(\omega_1, \omega_2) = \hat{\mathbf{R}} - \mathbf{G}(\omega_1, \omega_2)\mathbf{G}^H(\omega_1, \omega_1) \tag{74}$$

where

$$\mathbf{G}(\omega_1, \omega_2) = \frac{1}{\sqrt{2}}[\bar{\mathbf{g}}(\omega_1, \omega_2) \quad \tilde{\mathbf{g}}(\omega_1, \omega_2)]. \tag{75}$$

By observing (61), (69), and (70), we can show that $\hat{\mathbf{Q}}(\omega_1, \omega_2)$ is also persymmetric. Hence, (71) can be used to obtain $\hat{\alpha}_{\mathrm{APES}}(\omega_1, \omega_2)$ as

$$\hat{\alpha}_{\mathrm{APES}}(\omega_1, \omega_2) = \frac{\mathbf{a}^H_{M_1,M_2}(\omega_1, \omega_2)\hat{\mathbf{Q}}^{-1}(\omega_1, \omega_2)\bar{\mathbf{g}}(\omega_1, \omega_2)}{\mathbf{a}^H_{M_1,M_2}(\omega_1, \omega_2)\hat{\mathbf{Q}}^{-1}(\omega_1, \omega_2)\mathbf{a}_{M_1,M_2}(\omega_1, \omega_2)}. \tag{76}$$

Based on the 2-D extensions described above, it is not difficult to see that all the results of the previous section also hold true for the 2-D Capon and APES estimators. Indeed, as seen in Appendixes B and C, the proofs of these results are critically dependent only on the persymmetric property of the true and sample covariance matrices or, equivalently, the conjugate symmetry properties as shown in (9) and (61). Therefore, the proofs for the 2-D estimators follow the same pattern as those for the 1-D case, and thus, they are omitted.

## V. Numerical Examples

In the following, we study the Capon and APES complex amplitude estimates in a number of cases of interest. For both the 1-D and 2-D examples given below, we compare the performance of the forward-only Capon and APES as well as the forward-backward Capon and APES, which are, for simplicity, referred to as FCapon, FAPES, FBCapon, and FBAPES, respectively.

### *A. One-Dimensional Complex Spectral Estimation*

The 1-D data used in the examples consists of a sum of 15 complex sinusoids with the real and imaginary parts shown in Figs. 1(a) and (b), respectively, corrupted by a zero-mean complex white Gaussian noise. The data length is chosen as $N = 64$. In what follows, we are interested in the bias and variance properties of the estimators under study. The bias and variance results shown below correspond to the frequency of the first sinusoid, and they are obtained from 100 independent realizations.

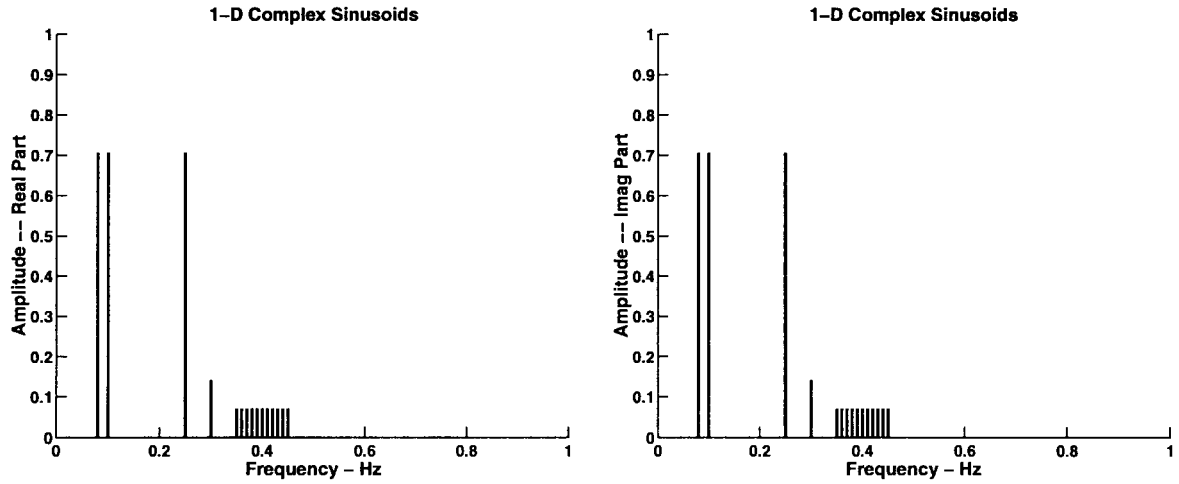


(a) (b)

Fig. 1. One-dimensional complex amplitude of the sum of 15 sinusoids used in the simulations. (a) Real part. (b) Imaginary part.

We begin by studying the performance of the estimators as the signal-to-noise ratio (SNR) varies. The SNR for the $k$th sinusoid is defined as

$$\mathrm{SNR}_k = 10\log_{10}\frac{\alpha_k^2}{P_e(\omega_k)}\ (\mathrm{dB}) \tag{77}$$

where $\alpha_k$ is the complex amplitude of the $k$th sinusoid, and $P_e(\omega_k)$ is the spectral density of the additive noise at frequency $\omega_k$. The filter length is chosen as $M = 15$. The real and imaginary parts of the bias are shown in Figs. 2(a) and (b), respectively, as a function of $\mathrm{SNR}_1$. As seen from these figures, FAPES and FBAPES are almost unbiased, whereas FCapon and FBCapon are biased downward. In addition, we notice that the bias for FCapon is approximately twice that of FBCapon. All these observations are consistent with the prediction of the theory. The variances of the real and imaginary parts of the amplitude estimates are shown in Figs. 2(c) and (d), respectively. It appears that all of the estimators display similar variances. However, as shown in the next example, the variance of Capon becomes notably larger than that of APES as $M$ increases.

Next, we study the effect of the filter length $M$ on the estimators. The $\mathrm{SNR}_1$ is fixed at 20 dB. As $M$ varies, the real and imaginary parts of the bias are shown in Figs. 3(a) and (b), respectively. From these figures, we can see that both FAPES and FBAPES are unbiased for all practical filter lengths, whereas the bias of Capon grows significantly with increasing $M$. (A *practical* filter length means that $M$ should not be too small [1]. In fact, all filterbank methods reduce to the Fourier transform approach when $M = 1$, and only when $M$ is sufficiently large, the filterbank approach shows noticeable improvement over the Fourier method [1].) All estimators seem to perform similarly for $M$ up to a fourth of the data length, with Capon being slightly biased downward. As the filter length increases further, the performance of Capon degrades rapidly, whereas that of APES remains unaffected. This observation is strengthened by the variance results shown for the real and imaginary parts of the amplitude estimates in Figs. 3(c) and (d), respectively.

It is known that as $M$ increases, all of the estimators under study achieve better spectral resolution and that the best resolution is obtained at $M = N/2$ [1]. This fact, along with the statistical results shown in the previous examples, indicates that the choice of $M$ for Capon should be made by a tradeoff between resolution and statistical stability. Usually, we choose $N/4 \leq M \leq N/2$. Although the choice of $M$ for Capon is difficult to make, it is easy to see that APES achieves the best performance at $M = N/2$ since with this choice, APES achieves the highest possible resolution as well as the best statistical properties in terms of bias and variance. The previous examples also show that FAPES and FBAPES perform similarly in terms of bias and variance properties for the frequency of interest.

To compare the computational complexities of the estimators under study, we count the flops required by each of them for the case, where $N = 64$, $M = 24$, and the complex spectra are evaluated at 256 equally spaced points. The flops required by FCapon and FBCapon are approximately the same, whereas the flops needed by FAPES and FBAPES are, respectively, 1.08 and 1.41 times of that by the Capon estimators.

### *B. Two-Dimensional Complex Spectral Estimation*

As was mentioned in Section IV, the 2-D Capon and APES estimators behave rather similarly to their 1-D counterparts. Since the problems encountered in applications such as synthetic aperture radar imaging are concerned with 2-D complex spectral estimation, we include a couple of 2-D numerical examples here. The data employed consists of three 2-D sinusoids corrupted by a 2-D zero-mean complex white Gaussian noise, with $N_1 = N_2 = 32$. The sinusoids are located in the frequency domain at $(0.2, 0.2), (0.25, 0.25)$ and $(0.4, 0.7)$, and their amplitudes are $e^{j\pi/4}, e^{j\pi/4}$ and $0.7e^{j\pi/4}$, respectively. The bias and variance for the amplitude estimate of the first 2-D sinusoid are obtained from 100 independent realizations. The SNR for the $k$th 2-D sinusoid is similarly defined as in (77). The bias and variance of the four estimators under study versus $\mathrm{SNR}_1$ are shown in Figs. 4(a) to (d),

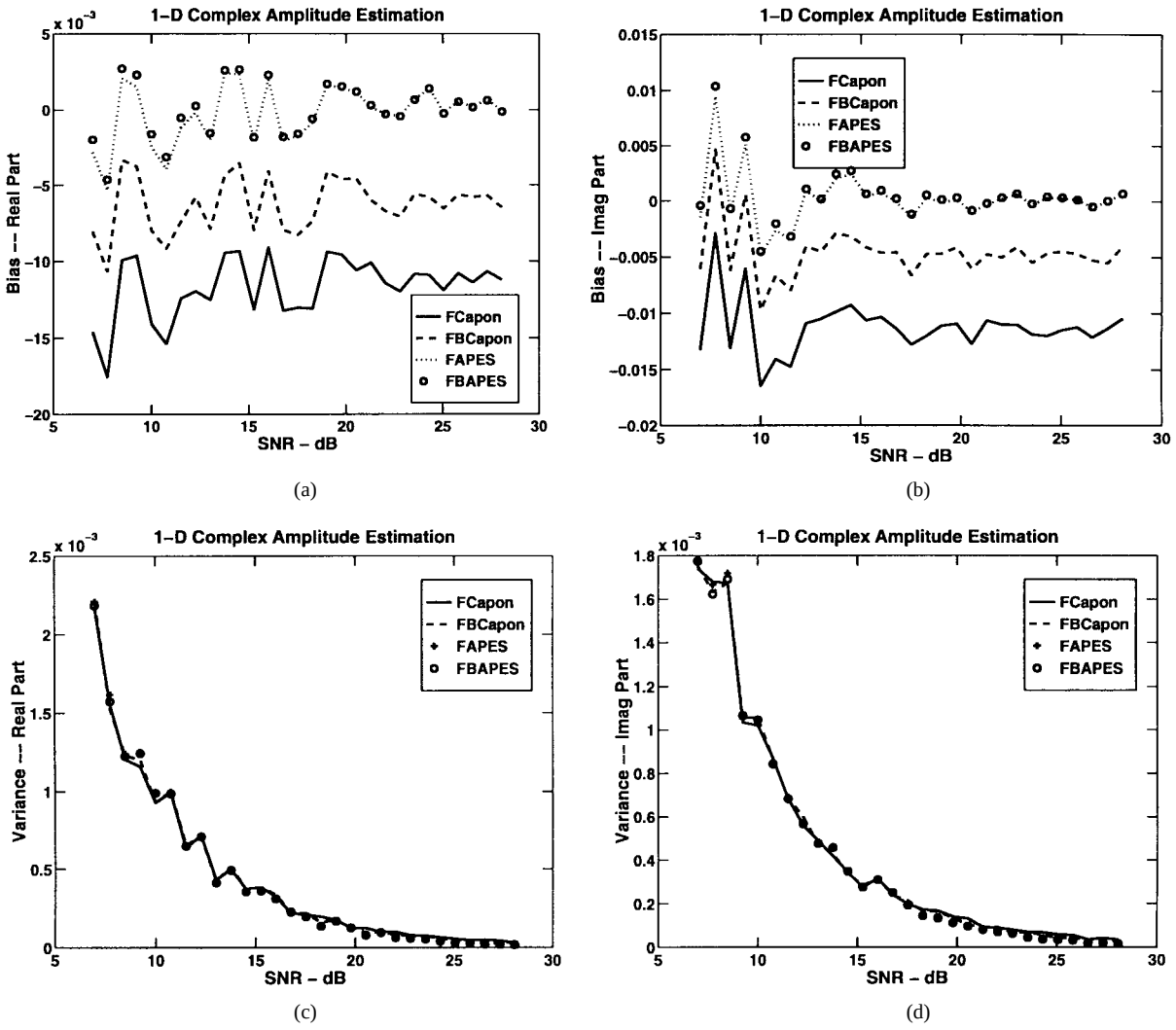


Fig. 2. Empirical bias and variance of the 1-D MAFI estimators as $\text{SNR}_1$ varies when $N = 64$ and $M = 15$. (a) Real part of the bias. (b) Imaginary part of the bias. (c) Variance of the real part of the estimated amplitude. (d) Variance of the imaginary part of the estimated amplitude.

respectively, where $M_1 = M_2 = 8$. Figs. 5(a) to (d) show the statistical results as the 2-D FIR filter length varies, where $\text{SNR}_1$ is fixed at 20 dB. We assume in Figs. 5(a) to (d) that $M_1 = M_2$. As seen from these plots, the performance of the 2-D MAFI estimators indeed resembles that of their 1-D counterparts, and therefore, we refer the readers to the 1-D examples for comments.

## VI. Conclusion

We have studied the forward-backward MAFI approaches to complex spectral estimation. The Capon and APES estimators are shown to belong to the class of the MAFI methods. By using a higher order expansion technique, we have proved that to within a second-order approximation, Capon is biased, whereas APES is unbiased and that the bias of the forward-backward Capon is half that of the forward-only Capon. We also show that all these conclusions carry over to the 2-D MAFI estimators. Since, computationally, APES is only slightly more involved than Capon, the preference of APES over Capon in practical applications follows logically because of the better statistical properties associated with the former.

## Appendix A
## Proof of (39)

The use of the MAFI filter given in (38) for spectral estimation requires an initial estimate of $\alpha(\omega)$. However, we can avoid that in the following way. By (25), the LS estimate of $\alpha(\omega)$ using the MAFI filter is given by

$$\hat{\alpha}_{\text{MAFI}}(\omega) = \mathbf{h}_\omega^H \bar{\mathbf{g}}(\omega) \tag{78}$$

where $\mathbf{h}_\omega$ is given by (38). Substituting (38) into (78), and after simple manipulations, we obtain

$$\begin{aligned}\Big[\mathbf{a}_M^H\hat{\mathbf{R}}^{-1}\mathbf{a}_M - \frac{1}{2}(\bar{\mathbf{g}}^H\hat{\mathbf{R}}^{-1}\bar{\mathbf{g}})(\mathbf{a}_M^H\hat{\mathbf{R}}^{-1}\mathbf{a}_M) \\ + \frac{1}{2}\left|\mathbf{a}_M^H\hat{\mathbf{R}}^{-1}\bar{\mathbf{g}}\right|^2\Big]\hat{\alpha}_{\text{MAFI}} + \Big[\frac{1}{2}(\mathbf{a}_M^H\hat{\mathbf{R}}^{-1}\bar{\mathbf{g}})(\tilde{\mathbf{g}}^H\hat{\mathbf{R}}^{-1}\mathbf{a}_M) \\ - \frac{1}{2}(\tilde{\mathbf{g}}^H\hat{\mathbf{R}}^{-1}\bar{\mathbf{g}})(\mathbf{a}_M^H\hat{\mathbf{R}}^{-1}\mathbf{a}_M)\Big]\hat{\bar{\alpha}}_{\text{MAFI}} = \mathbf{a}_M^H\hat{\mathbf{R}}^{-1}\bar{\mathbf{g}}\end{aligned} \tag{79}$$

where we, like before, omit the dependence on $\omega$ for notational simplicity. By borrowing the notations defined in (41)–(43),

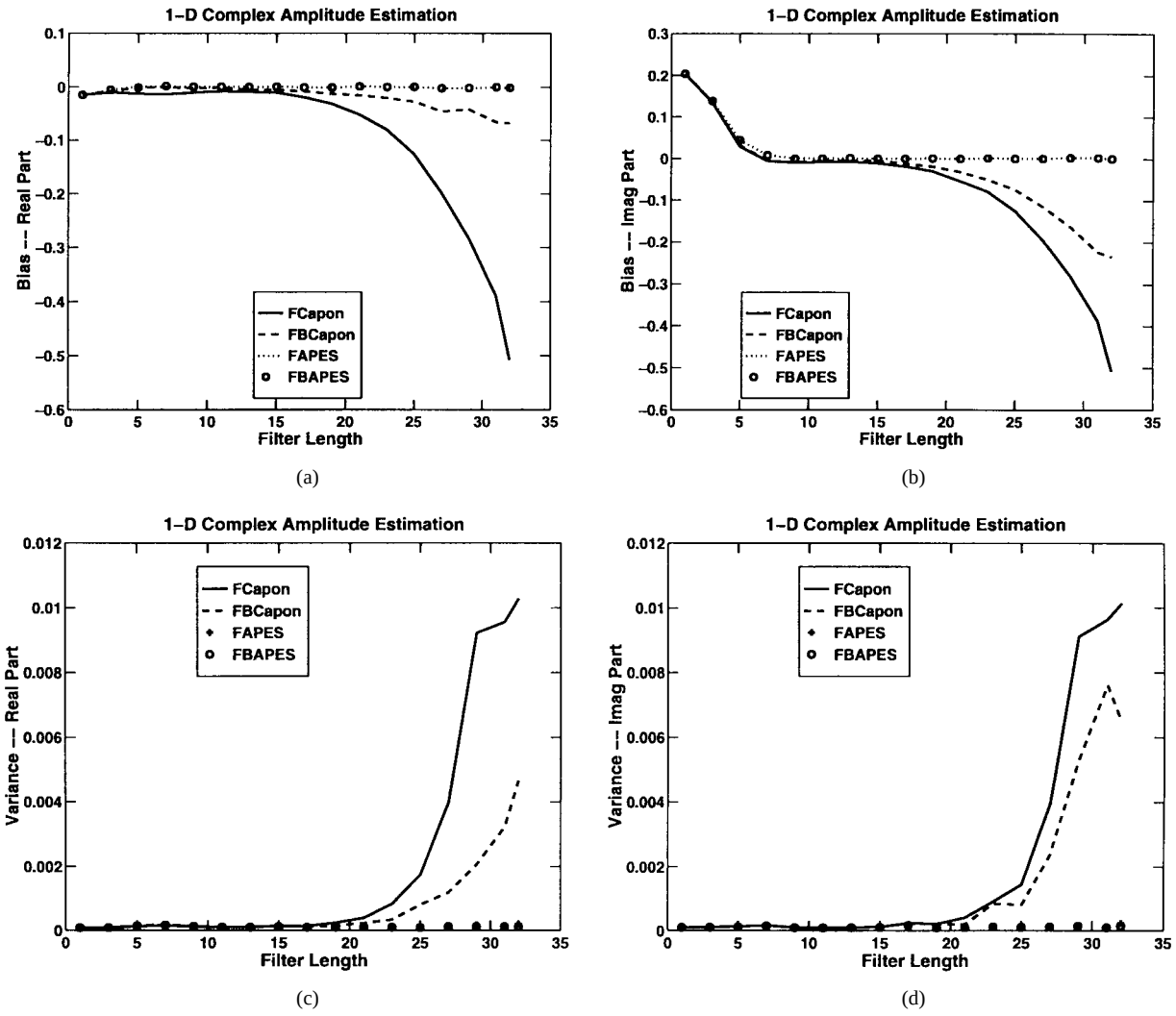


Fig. 3. Empirical bias and variance of the 1-D MAFI estimators as the filter length $M$ varies when $N = 64$ and $\mathrm{SRN}_1 = 20$ dB. (a) Real part of the bias. (b) Imaginary part of the bias. (c) Variance of the real part of the estimated amplitude. (d) Variance of the imaginary part of the estimated amplitude.

the solution $\hat{\alpha}_{\mathrm{MAFI}}$ to (79) is straightforward to obtain

$$\begin{aligned}\hat{\alpha}_{\mathrm{MAFI}} &= \Bigg[\nu_1^H\nu_2 - \frac{1}{2}\|\nu_3\|^2\left(\nu_1^H\nu_2\right) + \frac{1}{2}\left(\nu_1^H\nu_3\right)\left(\nu_2^H\nu_3\right)^*\Bigg] \Bigg/ \Bigg[\|\nu_1\|^2 - \frac{1}{2}\|\nu_1\|^2\|\nu_3\|^2 \\ &\quad + \frac{1}{2}\left|\nu_1^H\nu_3\right|^2 - \frac{1}{2}\|\nu_1\|^2\|\nu_2\|^2 + \frac{1}{4}\|\nu_1\|^2\|\nu_2\|^2\|\nu_3\|^3 \\ &\quad - \frac{1}{4}\|\nu_2\|^2\left|\nu_1^H\nu_3\right|^2 + \frac{1}{2}\left|\nu_1^H\nu_2\right|^2 - \frac{1}{4}\|\nu_3\|^3\left|\nu_1^H\nu_2\right|^2 \\ &\quad + \frac{1}{4}\left(\nu_1^H\nu_2\right)\left(\nu_1^H\nu_3\right)^*\left(\nu_2^H\nu_3\right) \\ &\quad + \frac{1}{4}\left(\nu_1^H\nu_2\right)^*\left(\nu_1^H\nu_3\right)\left(\nu_2^H\nu_3\right)^* - \frac{1}{4}\|\nu_1\|^2\left|\nu_2^H\nu_3\right|^2\Bigg].\end{aligned} \tag{80}$$

Next, we evaluate the APES estimator as given by (45). We first compute the $\Xi^{-1}$

$$\Xi^{-1} = \frac{2}{\Delta}\begin{bmatrix}\|\nu_3\|^2 - 2 & -\nu_2^H\nu_3 \\ -\left(\nu_2^H\nu_3\right)^* & \|\nu_2\|^2 - 2\end{bmatrix} \tag{81}$$

where

$$\Delta = \|\nu_2\|^2\|\nu_3\|^2 - 2\|\nu_2\|^2 - 2\|\nu_3\|^2 - \left|\nu_2^H\nu_3\right|^2 + 4. \tag{82}$$

Substituting (81) into (45) and performing some simple manipulations, we obtain

$$\begin{aligned}\hat{\alpha}_{\mathrm{APES}} &= \left[4\nu_1^H\nu_2 - 2\|\nu_3\|^2\left(\nu_1^H\nu_2\right) + 2\left(\nu_1^H\nu_3\right)\left(\nu_2^H\nu_3\right)^*\right] \Big/ \left[\|\nu_1\|^2\|\nu_2\|^2\|\nu_3\|^2 \right. \\ &\quad - 2\|\nu_1\|^2\|\nu_2\|^2 - 2\|\nu_1\|^2\|\nu_3\|^2 + 4\|\nu_1\|^2 \\ &\quad - \|\nu_1\|^2\left|\nu_2^H\nu_3\right|^2 - \|\nu_3\|^2\left|\nu_1^H\nu_2\right|^2 + 2\left|\nu_1^H\nu_2\right|^2 \\ &\quad \left. + \left(\nu_1^H\nu_2\right)^*\left(\nu_1^H\nu_3\right)\left(\nu_2^H\nu_3\right)^* + \left(\nu_1^H\nu_2\right)\left(\nu_1^H\nu_3\right)^*\left(\nu_2^H\nu_3\right) \right. \\ &\quad \left. - \|\nu_2\|^2\left|\nu_1^H\nu_3\right|^2 + 2\left|\nu_1^H\nu_3\right|^2\right].\end{aligned} \tag{83}$$

Comparing (80) and (83) confirms that APES and MAFI coincide. □

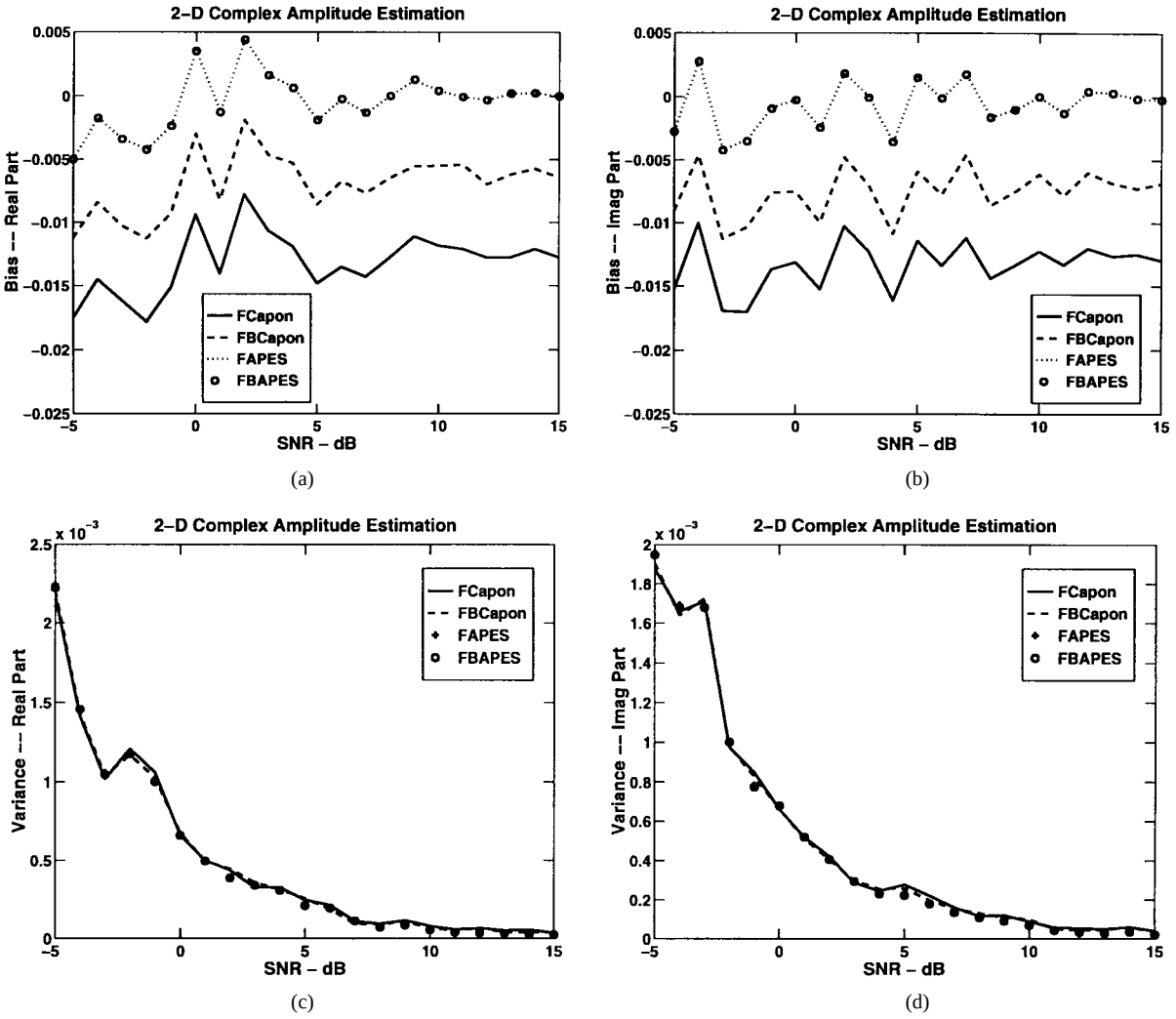


Fig. 4. Empirical bias and variance of the 2-D MAFI estimators as $\text{SNR}_1$ varies when $N_1 = N_2 = 32$ and $M_1 = M_2 = 8$. (a) Real part of the bias. (b) Imaginary part of the bias. (c) Variance of the real part of the estimated amplitude. (d) Variance of the imaginary part of the estimated amplitude.

## APPENDIX B
## PROOF OF THEOREM 1

From (4) and (7), we have

$$\bar{\mathbf{g}} = \alpha \mathbf{a}_M + \bar{\boldsymbol{\delta}} \tag{84}$$

$$\tilde{\mathbf{g}} = \tilde{\alpha} \mathbf{a}_M + \tilde{\boldsymbol{\delta}} \tag{85}$$

where $\bar{\boldsymbol{\delta}}$ and $\tilde{\boldsymbol{\delta}}$, respectively, are defined as

$$\bar{\boldsymbol{\delta}} = \frac{1}{L} \sum_{l=0}^{L-1} \bar{\mathbf{e}}_\omega(l) e^{-j\omega l} \tag{86}$$

$$\tilde{\boldsymbol{\delta}} = \frac{1}{L} \sum_{l=0}^{L-1} \tilde{\mathbf{e}}_\omega(l) e^{-j\omega l}. \tag{87}$$

First, we calculate the first- and second-order moments of $\bar{\boldsymbol{\delta}}$ and $\tilde{\boldsymbol{\delta}}$

$$E\{\bar{\boldsymbol{\delta}}\} = \mathbf{0} \tag{88}$$

$$E\{\tilde{\boldsymbol{\delta}}\} = \mathbf{0} \tag{89}$$

$$E\{\bar{\boldsymbol{\delta}}\bar{\boldsymbol{\delta}}^T\} = \mathbf{0} \tag{90}$$

$$E\{\tilde{\boldsymbol{\delta}}\tilde{\boldsymbol{\delta}}^T\} = \mathbf{0} \tag{91}$$

$$\begin{aligned} E\{\bar{\boldsymbol{\delta}}\bar{\boldsymbol{\delta}}^H\} &= \frac{1}{L^2} \sum_{l=0}^{L-1} \sum_{k=0}^{L-1} E\{\bar{\mathbf{e}}_\omega(l) \bar{\mathbf{e}}_\omega^H(k)\} e^{-j\omega(l-k)} \\ &= \frac{1}{L^2} \sum_{i=-(L-1)}^{L-1} (L - |i|) \mathbf{R}_e(i) e^{-j\omega i} \end{aligned} \tag{92}$$

$$\begin{aligned} E\{\tilde{\boldsymbol{\delta}}\tilde{\boldsymbol{\delta}}^H\} &= \frac{1}{L^2} \sum_{l=0}^{L-1} \sum_{k=0}^{L-1} E\{\tilde{\mathbf{e}}_\omega(l) \tilde{\mathbf{e}}_\omega^H(k)\} e^{-j\omega(l-k)} \\ &= \frac{1}{L^2} \sum_{i=-(L-1)}^{L-1} (L - |i|) \mathbf{R}_e(i) e^{-j\omega i} \end{aligned} \tag{93}$$

where $\{\mathbf{R}_e(i)\}$ is the covariance sequence of $\bar{\mathbf{e}}_\omega(l)$ or $\tilde{\mathbf{e}}_\omega(l)$. Note that (90) and (91) are due to the circularly symmetric distribution assumption. It then follows from (92), (93), and Condition **C** that

$$\begin{aligned} \lim_{L\to\infty} LE\{\bar{\boldsymbol{\delta}}\bar{\boldsymbol{\delta}}^H\} &= \lim_{L\to\infty} LE\{\tilde{\boldsymbol{\delta}}\tilde{\boldsymbol{\delta}}^H\} \\ &= \sum_{i=-\infty}^{\infty} \mathbf{R}_e(i) e^{-j\omega i} = P_e(\omega) \mathbf{a}_M \mathbf{a}_M^H \end{aligned} \tag{94}$$

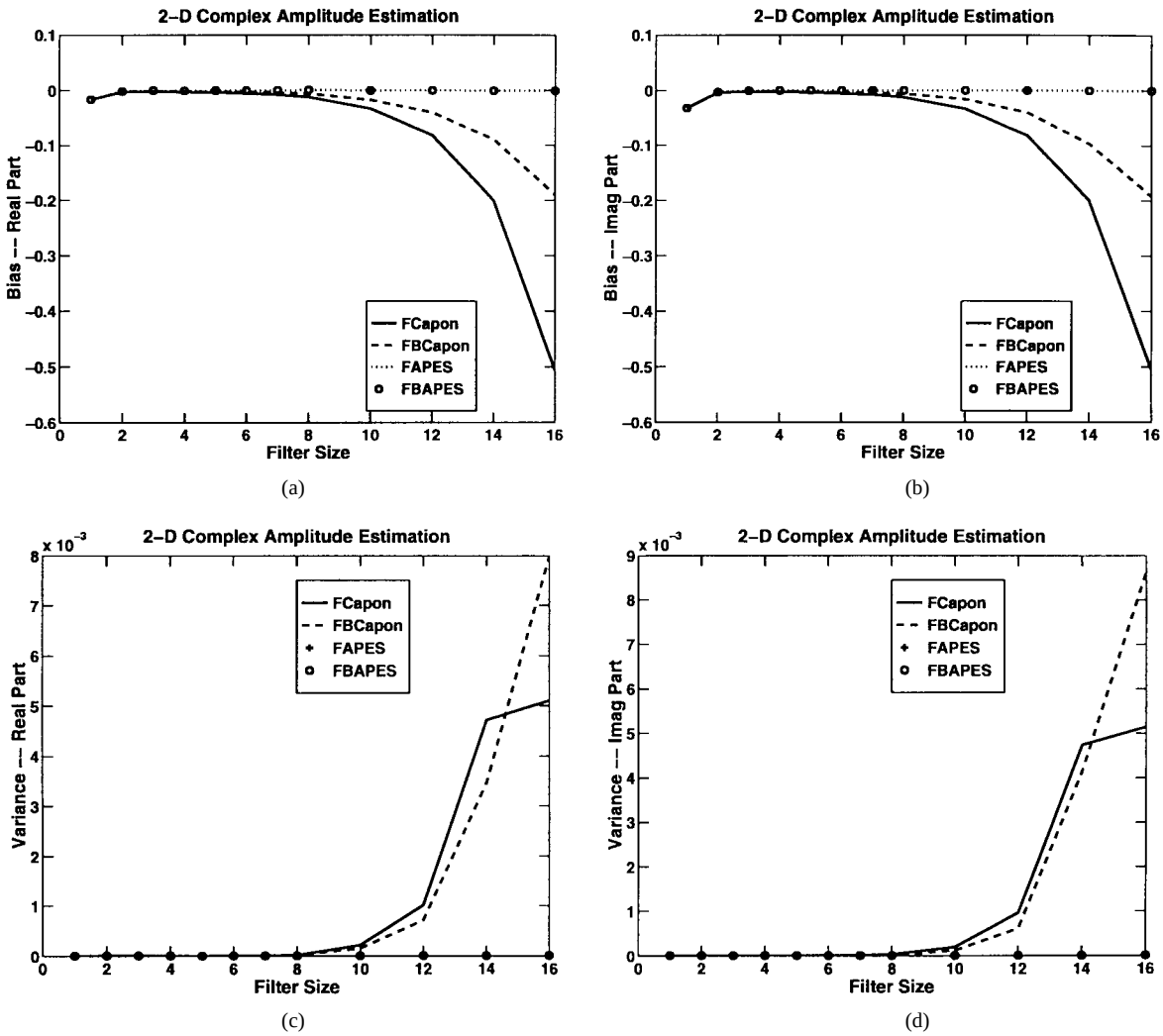


Fig. 5. Empirical bias and variance of the 2-D MAFI estimators as the filter length $M = M_1 = M_2$ varies when $N_1 = N_2 = 32$, and $\text{SRN}_1 = 20$ dB. (a) Real part of the bias. (b) Imaginary part of the bias. (c) Variance of the real part of the estimated amplitude. (d) Variance of the imaginary part of the estimated amplitude.

where the last equality follows from the standard results on the transfer of spectral densities through linear systems. Among others, the previous calculations imply that as $L \to \infty, \hat{\mathbf{g}}$ and $\tilde{\mathbf{g}}$ tend to $\alpha \mathbf{a}_M$ and $\tilde{\alpha}\mathbf{a}_M$ (in the mean square sense), respectively. $\mathbf{G}\mathbf{G}^H$, therefore, goes to $|\alpha|^2 \mathbf{a}_M \mathbf{a}_M^H$. Hence, $\mathbf{h}_\omega^{\text{Capon}}$ and $\mathbf{h}_\omega^{\text{APES}}$ have the same limit as $L \to \infty$.

Let $\mathbf{h}$ denote a generic FIR vector, and let $\mathbf{h}_\infty$ denote the deterministic vector that is the limit of (the possibly random) $\mathbf{h}$ when $L$ goes to infinity. Observe that for all methods under study, the associated $\mathbf{h}$ and $\mathbf{h}_\infty$ vectors satisfy

$$\mathbf{h}^H \mathbf{a}_M = 1, \quad \text{and} \quad \mathbf{h}_\infty^H \mathbf{a}_M = 1. \tag{95}$$

By using this observation with (25) and (84), we obtain

$$\hat{\alpha} = \mathbf{h}^H \bar{\mathbf{g}} = \alpha + \mathbf{h}^H \bar{\boldsymbol{\delta}}. \tag{96}$$

Since $\bar{\boldsymbol{\delta}}$ tends to zero as $L$ goes to infinity, it follows from (96) that the estimation error can be asymptotically written as (to a *first-order* approximation)

$$\hat{\alpha} - \alpha \simeq \mathbf{h}_\infty^H \bar{\boldsymbol{\delta}}. \tag{97}$$

Then, it readily follows that

$$LE\{(\hat{\alpha} - \alpha)^2\} = 0, \quad \text{as } L \to \infty \tag{98}$$

and

$$\begin{aligned} \lim_{L\to\infty} LE\{|\hat{\alpha} - \alpha|^2\} &= \mathbf{h}_\infty^H \lim_{L\to\infty} LE\{\bar{\boldsymbol{\delta}}\bar{\boldsymbol{\delta}}^H\}\mathbf{h}_\infty \\ &= P_e(\omega)\left|\mathbf{h}_\infty^H \mathbf{a}_M\right|^2 = P_e(\omega) \end{aligned} \tag{99}$$

and the proof is concluded. □

## APPENDIX C
## PROOF OF THEOREM 2

*Proof of (49):* By using (27) and (96), we obtain

$$\hat{\alpha}_{\text{Capon}} - \alpha = \frac{\mathbf{a}_M^H \hat{\mathbf{R}}^{-1} \bar{\boldsymbol{\delta}}}{\mathbf{a}_M^H \hat{\mathbf{R}}^{-1} \mathbf{a}_M}. \tag{100}$$

In what follows, we use the symbol $\approx$ to denote an "asymptotic equality" that holds to within a *second-order* approximation.

A straightforward manipulation of (100) yields

$$\begin{aligned}
&\hat{\alpha}_{\text{Capon}} - \alpha \\
&\quad = \frac{\mathbf{a}_M^H(\hat{\mathbf{R}}^{-1} - \mathbf{R}^{-1})\bar{\boldsymbol{\delta}}}{\mathbf{a}_M^H\hat{\mathbf{R}}^{-1}\mathbf{a}_M} + \frac{\mathbf{a}_M^H\mathbf{R}^{-1}\bar{\boldsymbol{\delta}}}{\mathbf{a}_M^H\hat{\mathbf{R}}^{-1}\mathbf{a}_M} \\
&\quad = \frac{\mathbf{a}_M^H\hat{\mathbf{R}}^{-1}(\mathbf{R} - \hat{\mathbf{R}})\mathbf{R}^{-1}\bar{\boldsymbol{\delta}}}{\mathbf{a}_M^H\hat{\mathbf{R}}^{-1}\mathbf{a}_M} + \mathbf{a}_M^H\mathbf{R}^{-1}\bar{\boldsymbol{\delta}} \\
&\qquad \times \left[\frac{1}{\mathbf{a}_M^H\hat{\mathbf{R}}^{-1}\mathbf{a}_M} - \frac{1}{\mathbf{a}_M^H\mathbf{R}^{-1}\mathbf{a}_M} + \frac{1}{\mathbf{a}_M^H\mathbf{R}^{-1}\mathbf{a}_M}\right] \\
&\quad \approx -\frac{\mathbf{a}_M^H\mathbf{R}^{-1}(\hat{\mathbf{R}} - \mathbf{R})\mathbf{R}^{-1}\bar{\boldsymbol{\delta}}}{\mathbf{a}_M^H\mathbf{R}^{-1}\mathbf{a}_M} + \frac{\mathbf{a}_M^H\mathbf{R}^{-1}\bar{\boldsymbol{\delta}}}{\mathbf{a}_M^H\mathbf{R}^{-1}\mathbf{a}_M} \\
&\qquad + \frac{\mathbf{a}_M^H\mathbf{R}^{-1}\bar{\boldsymbol{\delta}}\mathbf{a}_M^H(\mathbf{R}^{-1} - \hat{\mathbf{R}}^{-1})\mathbf{a}_M}{\big(\mathbf{a}_M^H\hat{\mathbf{R}}^{-1}\mathbf{a}_M\big)\big(\mathbf{a}_M^H\mathbf{R}^{-1}\mathbf{a}_M\big)} \\
&\quad \approx -\frac{\mathbf{a}_M^H\mathbf{R}^{-1}(\hat{\mathbf{R}} - \mathbf{R})\mathbf{R}^{-1}\bar{\boldsymbol{\delta}}}{\mathbf{a}_M^H\mathbf{R}^{-1}\mathbf{a}_M} + \frac{\mathbf{a}_M^H\mathbf{R}^{-1}\bar{\boldsymbol{\delta}}}{\mathbf{a}_M^H\mathbf{R}^{-1}\mathbf{a}_M} \\
&\qquad + \frac{\big(\mathbf{a}_M^H\mathbf{R}^{-1}\bar{\boldsymbol{\delta}}\big)\mathbf{a}_M^H\mathbf{R}^{-1}(\hat{\mathbf{R}} - \mathbf{R})\mathbf{R}^{-1}\mathbf{a}_M}{\big(\mathbf{a}_M^H\mathbf{R}^{-1}\mathbf{a}_M\big)^2} \qquad (101)
\end{aligned}$$

which, in turn, implies (102), shown at the bottom of the page. Next, we note that

$$\begin{aligned}
\hat{\mathbf{R}} &= \frac{1}{2L}\sum_{l=0}^{L-1}\big[\big(\alpha\mathbf{a}_M e^{j\omega l} + \bar{\mathbf{e}}(l)\big)\big(\alpha\mathbf{a}_M e^{j\omega l} + \bar{\mathbf{e}}(l)\big)^H \\
&\quad + \big(\tilde{\alpha}\mathbf{a}_M e^{j\omega l} + \tilde{\mathbf{e}}(l)\big)\big(\tilde{\alpha}\mathbf{a}_M e^{j\omega l} + \tilde{\mathbf{e}}(l)\big)^H\big] \\
&= |\alpha|^2\mathbf{a}_M\mathbf{a}_M^H + \frac{1}{2}(\alpha^*\bar{\boldsymbol{\delta}} + \tilde{\alpha}^*\tilde{\boldsymbol{\delta}})\mathbf{a}_M^H + \frac{1}{2}\mathbf{a}_M(\alpha\bar{\boldsymbol{\delta}}^H + \tilde{\alpha}\tilde{\boldsymbol{\delta}}^H) \\
&\quad + \frac{1}{2L}\sum_{l=0}^{L-1}\big[\bar{\mathbf{e}}_\omega(l)\bar{\mathbf{e}}_\omega^H(l) + \tilde{\mathbf{e}}_\omega(l)\tilde{\mathbf{e}}_\omega^H(l)\big]. \qquad (103)
\end{aligned}$$

We also recall (88) and the assumption that $\bar{\mathbf{e}}_\omega(n)$ and $\tilde{\mathbf{e}}_\omega(n)$ have zero third-order moments. Since

$$\tilde{\mathbf{e}}_\omega(l) = \mathbf{J}\bar{\mathbf{e}}_\omega^*(L - l - 1) \qquad (104)$$

which is like (9), we have

$$\begin{aligned}
\tilde{\boldsymbol{\delta}} &= \frac{1}{L}\sum_{l=0}^{L-1}\tilde{\mathbf{e}}_\omega(l)e^{-j\omega l} = \frac{1}{L}\sum_{l=0}^{L-1}\mathbf{J}\bar{\mathbf{e}}_\omega^*(L - l - 1)e^{-j\omega l} \\
&= e^{-j\omega(L-1)}\mathbf{J}\left[\frac{1}{L}\sum_{k=0}^{L-1}\tilde{\mathbf{e}}_\omega(k)e^{-j\omega k}\right]^* = e^{-j\omega(L-1)}\mathbf{J}\bar{\boldsymbol{\delta}}^*. \qquad (105)
\end{aligned}$$

By using these facts, along with (102), we can write

$$\begin{aligned}
&\big(\mathbf{a}_M^H\mathbf{R}^{-1}\mathbf{a}_M\big)^2 E\{\hat{\alpha}_{\text{Capon}} - \alpha\} \\
&\quad \approx E\Big\{\big(\mathbf{a}_M^H\mathbf{R}^{-1}\mathbf{a}_M\big)\Big[-\frac{1}{2}\mathbf{a}_M^H\mathbf{R}^{-1}(\alpha^*\bar{\boldsymbol{\delta}} + \tilde{\alpha}^*\tilde{\boldsymbol{\delta}})\big(\mathbf{a}_M^H\mathbf{R}^{-1}\bar{\boldsymbol{\delta}}\big) \\
&\qquad - \frac{1}{2}\big(\mathbf{a}_M^H\mathbf{R}^{-1}\mathbf{a}_M\big)(\alpha\bar{\boldsymbol{\delta}}^H + \tilde{\alpha}\tilde{\boldsymbol{\delta}}^H)\mathbf{R}^{-1}\bar{\boldsymbol{\delta}}\Big] \\
&\qquad + \big(\mathbf{a}_M^H\mathbf{R}^{-1}\bar{\boldsymbol{\delta}}\big)\Big[\frac{1}{2}\mathbf{a}_M^H\mathbf{R}^{-1}(\alpha^*\bar{\boldsymbol{\delta}} + \tilde{\alpha}^*\tilde{\boldsymbol{\delta}})\big(\mathbf{a}_M^H\mathbf{R}^{-1}\mathbf{a}_M\big) \\
&\qquad + \frac{1}{2}\big(\mathbf{a}_M^H\mathbf{R}^{-1}\mathbf{a}_M\big)(\alpha\bar{\boldsymbol{\delta}}^H + \tilde{\alpha}\tilde{\boldsymbol{\delta}}^H)\mathbf{R}^{-1}\mathbf{a}_M\Big]\Big\} \\
&\quad = \frac{1}{2}E\big\{\alpha^*\big(\mathbf{a}_M^H\mathbf{R}^{-1}\bar{\boldsymbol{\delta}}\big)^2\big(\mathbf{a}_M^H\mathbf{R}^{-1}\mathbf{a}_M\big) \\
&\qquad + \tilde{\alpha}^*\big(\mathbf{a}_M^H\mathbf{R}^{-1}\bar{\boldsymbol{\delta}}\big)\big(\mathbf{a}_M^H\mathbf{R}^{-1}\tilde{\boldsymbol{\delta}}\big)\big(\mathbf{a}_M^H\mathbf{R}^{-1}\mathbf{a}_M\big) \\
&\qquad + \alpha\big(\mathbf{a}_M^H\mathbf{R}^{-1}\mathbf{a}_M\big)\big|\mathbf{a}_M^H\mathbf{R}^{-1}\hat{\boldsymbol{\delta}}\big|^2 \\
&\qquad + \tilde{\alpha}\big(\mathbf{a}_M^H\mathbf{R}^{-1}\mathbf{a}_M\big)\big(\mathbf{a}_M^H\mathbf{R}^{-1}\bar{\boldsymbol{\delta}}\big)\big(\tilde{\boldsymbol{\delta}}^H\mathbf{R}^{-1}\mathbf{a}_M\big) \\
&\qquad - \alpha^*\big(\mathbf{a}_M^H\mathbf{R}^{-1}\mathbf{a}_M\big)\big(\mathbf{a}_M^H\mathbf{R}^{-1}\bar{\boldsymbol{\delta}}\big)^2 \\
&\qquad - \tilde{\alpha}^*\big(\mathbf{a}_M^H\mathbf{R}^{-1}\mathbf{a}_M\big)\big(\mathbf{a}_M^H\mathbf{R}^{-1}\tilde{\boldsymbol{\delta}}\big)\big(\mathbf{a}_M^H\mathbf{R}^{-1}\bar{\boldsymbol{\delta}}\big) \\
&\qquad - \alpha\big(\mathbf{a}_M^H\mathbf{R}^{-1}\mathbf{a}_M\big)^2(\bar{\boldsymbol{\delta}}^H\mathbf{R}^{-1}\bar{\boldsymbol{\delta}}) \\
&\qquad - \tilde{\alpha}\big(\mathbf{a}_M^H\mathbf{R}^{-1}\mathbf{a}_M\big)^2(\tilde{\boldsymbol{\delta}}^H\mathbf{R}^{-1}\bar{\boldsymbol{\delta}})\big\} \\
&\quad = \frac{1}{2}\alpha\big(\mathbf{a}_M^H\mathbf{R}^{-1}\mathbf{a}_M\big)E\big\{\big|\mathbf{a}_M^H\mathbf{R}^{-1}\bar{\boldsymbol{\delta}}\big|^2 \\
&\qquad - \big(\mathbf{a}_M^H\mathbf{R}^{-1}\mathbf{a}_M\big)(\bar{\boldsymbol{\delta}}^H\mathbf{R}^{-1}\bar{\boldsymbol{\delta}})\big\}. \qquad (106)
\end{aligned}$$

By the Cauchy-Schwartz inequality, the quantity between the curly parentheses in (106) is negative and so is its expectation. Hence, (49) follows.

The bias for the forward-only Capon spectral estimate $\hat{\tilde{\alpha}}_{\text{Capon}}$ can be obtained by replacing the forward-backward sample covariance $\hat{\mathbf{R}}$ in (100)–(102) by the forward-only sample covariance matrix $\hat{\tilde{\mathbf{R}}}$, as defined in (12), and by following a similar treatment we did in (106). The result is (to a second-order approximation)

$$\begin{aligned}
&\big(\mathbf{a}_M^H\mathbf{R}^{-1}\mathbf{a}_M\big)^2 E\{\hat{\tilde{\alpha}}_{\text{Capon}} - \alpha\} \\
&\quad \approx \alpha\big(\mathbf{a}_M^H\mathbf{R}^{-1}\mathbf{a}_M\big)E\big\{\big|\mathbf{a}_M^H\mathbf{R}^{-1}\bar{\boldsymbol{\delta}}\big|^2 \\
&\qquad - \big(\mathbf{a}_M^H\mathbf{R}^{-1}\mathbf{a}_M\big)(\bar{\boldsymbol{\delta}}^H\mathbf{R}^{-1}\bar{\boldsymbol{\delta}})\big\}. \qquad (107)
\end{aligned}$$

Hence, to within a second-order approximation, the bias of the forward-backward Capon is indeed one half that of the forward-only Capon. □

*Proof of (50):* By making use of the fact that $\hat{\mathbf{Q}}^{\text{APES}} - \mathbf{Q} = O(1/\sqrt{L})$, (50) can be proved similarly to (49). By (33) and

$$E\{\hat{\alpha}_{\text{Capon}} - \alpha\} \approx E\left\{\frac{-\big(\mathbf{a}_M^H\mathbf{R}^{-1}\hat{\mathbf{R}}\mathbf{R}^{-1}\bar{\boldsymbol{\delta}}\big)\big(\mathbf{a}_M^H\mathbf{R}^{-1}\mathbf{a}_M\big) + \big(\mathbf{a}_M^H\mathbf{R}^{-1}\hat{\mathbf{R}}\mathbf{R}^{-1}\mathbf{a}_M\big)\big(\mathbf{a}_M^H\mathbf{R}^{-1}\bar{\boldsymbol{\delta}}\big)}{\big(\mathbf{a}_M^H\mathbf{R}^{-1}\mathbf{a}_M\big)^2}\right\}. \qquad (102)$$

(96), we have

$$\hat{\alpha}_{\mathrm{APES}} - \alpha = \frac{\mathbf{a}_M^H \hat{\mathbf{Q}}^{-1} \bar{\boldsymbol{\delta}}}{\mathbf{a}_M^H \hat{\mathbf{Q}}^{-1} \mathbf{a}_M} \approx -\frac{\mathbf{a}_M^H \mathbf{Q}^{-1} (\hat{\mathbf{Q}} - \mathbf{Q}) \mathbf{Q}^{-1} \bar{\boldsymbol{\delta}}}{\mathbf{a}_M^H \mathbf{Q}^{-1} \mathbf{a}_M} + \frac{\mathbf{a}_M^H \mathbf{Q}^{-1} \bar{\boldsymbol{\delta}}}{\mathbf{a}_M^H \mathbf{Q}^{-1} \mathbf{a}_M} + \frac{\left(\mathbf{a}_M^H \mathbf{Q}^{-1} \bar{\boldsymbol{\delta}}\right) \mathbf{a}_M^H \mathbf{Q}^{-1} (\hat{\mathbf{Q}} - \mathbf{Q}) \mathbf{Q}^{-1} \mathbf{a}_M}{\left(\mathbf{a}_M^H \mathbf{Q}^{-1} \mathbf{a}_M\right)^2}. \tag{108}$$

Therefore, we obtain

$$\left(\mathbf{a}_M^H \mathbf{Q}^{-1} \mathbf{a}_M\right)^2 E\{\hat{\alpha}_{\mathrm{APES}} - \alpha\} \approx E\{-\left(\mathbf{a}_M^H \mathbf{Q}^{-1} \hat{\mathbf{Q}} \mathbf{Q}^{-1} \bar{\boldsymbol{\delta}}\right)\left(\mathbf{a}_M^H \mathbf{Q}^{-1} \mathbf{a}_M\right) + \left(\mathbf{a}_M^H \mathbf{Q}^{-1} \hat{\mathbf{Q}} \mathbf{Q}^{-1} \mathbf{a}_M\right)\left(\mathbf{a}_M^H \mathbf{Q}^{-1} \bar{\boldsymbol{\delta}}\right)\}. \tag{109}$$

Next, note that

$$\begin{aligned}\hat{\mathbf{Q}} &= \hat{\mathbf{R}} - \mathbf{G}\mathbf{G}^H = \hat{\mathbf{R}} - \frac{1}{2}[\bar{\mathbf{g}}\bar{\mathbf{g}}^H + \tilde{\mathbf{g}}\tilde{\mathbf{g}}^H] \\ &= |\alpha|^2 \mathbf{a}_M \mathbf{a}_M^H + \frac{1}{2}\alpha^* \bar{\boldsymbol{\delta}} \mathbf{a}_M^H + \frac{1}{2}\tilde{\alpha}^* \tilde{\boldsymbol{\delta}} \mathbf{a}_M^H + \frac{1}{2}\alpha \mathbf{a}_M \bar{\boldsymbol{\delta}}^H \\ &\quad + \frac{1}{2}\tilde{\alpha} \mathbf{a}_M \tilde{\boldsymbol{\delta}}^H + \frac{1}{2L}\sum_{l=0}^{L-1}\left[\bar{\mathbf{e}}_\omega(l)\bar{\mathbf{e}}_\omega^H(l) + \tilde{\mathbf{e}}_\omega(l)\tilde{\mathbf{e}}_\omega^H(l)\right] \\ &\quad - |\alpha|^2 \mathbf{a}_M \mathbf{a}_M^H - \frac{1}{2}\alpha \mathbf{a}_M \bar{\boldsymbol{\delta}}^H - \frac{1}{2}\alpha^* \bar{\boldsymbol{\delta}} \mathbf{a}_M^H \\ &\quad - \frac{1}{2}\tilde{\alpha} \mathbf{a}_M \tilde{\boldsymbol{\delta}}^H - \frac{1}{2}\tilde{\alpha}^* \tilde{\boldsymbol{\delta}} \mathbf{a}_M^H - \frac{1}{2}[\bar{\boldsymbol{\delta}}\bar{\boldsymbol{\delta}}^H + \tilde{\boldsymbol{\delta}}\tilde{\boldsymbol{\delta}}^H] \\ &= \frac{1}{2L}\sum_{l=0}^{L-1}\left[\bar{\mathbf{e}}_\omega(l)\bar{\mathbf{e}}_\omega^H(l) + \tilde{\mathbf{e}}_\omega(l)\tilde{\mathbf{e}}_\omega^H(l)\right] \\ &\quad - \frac{1}{2}[\bar{\boldsymbol{\delta}}\bar{\boldsymbol{\delta}}^H + \tilde{\boldsymbol{\delta}}\tilde{\boldsymbol{\delta}}^H]\end{aligned} \tag{110}$$

where we have made use of (103) and (84) and (85). Using again the assumption of zero third-order moments of $\bar{\mathbf{e}}_\omega(n)$ and $\tilde{\mathbf{e}}_\omega(n)$, and combining (109) and (110) yields (to a second-order approximation)

$$E\{\hat{\alpha}_{\mathrm{APES}} - \alpha\} \approx 0 \tag{111}$$

and the proof is complete.

To motivate the normalizing factor $L$ used in both (49) and (50), we mention the fact that both $\bar{\boldsymbol{\delta}}$ and $\tilde{\boldsymbol{\delta}}$ are $O(1/\sqrt{L})$, and this implies that the second-order approximation previously used for both $E\{\hat{\alpha}_{\mathrm{Capon}} - \alpha\}$ and $E\{\hat{\alpha}_{\mathrm{APES}} - \alpha\}$ is $O(1/L)$.

## REFERENCES


[1] J. Li and P. Stoica, "An adaptive filtering approach to spectral estimation and SAR imaging," *IEEE Trans. Signal Processing*, vol. 44, pp. 1469–1484, June 1996.

[2] J. Capon, "High resolution frequency-wavenumber spectrum analysis," *Proc. IEEE*, vol. 57, pp. 1408–1418, Aug. 1969.

[3] R. T. Lacoss, "Data adaptive spectral analysis methods," *Geophys.*, vol. 36, pp. 661–675, Aug. 1971.

[4] P. Stoica, A. Jakobsson, and J. Li, "Matched-filter bank interpretation of some spectral estimators," *Signal Process.*, vol. 66, no. 1, 1998.

[5] S. M. Kay, *Modern Spectral Estimation: Theory and Application*, Englewood Cliffs, NJ: Prentice-Hall, 1988.

[6] G. H. Golub and C. F. Van Loan, *Matrix Computations*. Baltimore, MD: Johns Hopkins Univ. Press, 1996.

[7] P. Stoica and R. L. Moses, *Introduction to Spectral Analysis*. Upper Saddle River, NJ: Prentice Hall, 1997.

[8] Z.-S. Liu, H. Li, and J. Li, "Efficient implementation of Capon and APES for spectral estimation," *IEEE Aerosp. Electron. Syst.*, to be published.



**Hongbin Li** (S'98) received the B.S. degree in 1991 and M.S. degree in 1994 from the University of Electronic Science and Technology of China (UESTC), Chengdu, all in electrical engineering. He is currently pursuing the Ph.D. degree in electrical engineering at the University of Florida, Gainesville

From 1994 to 1995, he was an Assistant Lecturer at UESTC. Since 1996, he has been a Research Assistant in the Department of Electrical and Computer Engineering at the University of Florida. His current research interests include digital signal processing, detection and estimation theory, and communications.

Mr. Li is a member of Tau Beta Pi.



**Jian Li** (S'87–M'91–SM'97) received the M.Sc. and Ph.D. degrees in electrical engineering from The Ohio State University, Columbus, in 1987 and 1991, respectively.

From April 1991 to June 1991, she was an Adjunct Assistant Professor with the Department of Electrical Engineering, The Ohio State University. From July 1991 to June 1993, she was an Assistant Professor with the Department of Electrical Engineering, University of Kentucky, Lexington. Since August 1993, she has been with the Department of Electrical and Computer Engineering, University of Florida, Gainesville, where she is currently an Associate Professor. Her current research interests include spectral estimation, synthetic aperture radar image formation and understanding, radar detection and estimation theory, sensor array signal processing, image segmentation and processing, and communications.

Dr. Li is a member of Sigma Xi and Phi Kappa Phi. She received the 1994 National Science Foundation Young Investigator Award and the 1996 Office of Naval Research Young Investigator Award.



**Petre Stoica** (F'94) received the M.Sc. and D.Sc. degrees, both in automatic control, from the Bucharest Polytechnic Institute, Bucharest, Romania, in 1972 and 1979, respectively. In 1993, he was awarded an Honorary Doctorate from Uppsala University, Uppsala, Sweden.

Since 1972, he has been with the Department of Automatic Control and Computers, Polytechnic Institute of Bucharest, where he holds the position of Professor of System Identification and Signal Processing. He spent 1992, 1993, and the first half of 1994 with the Systems and Control Group, Uppsala University, as a Guest Professor. In the second half of 1994, he held a Chalmers 150th Anniversary Visiting Professorship with the Applied Electronics Department, Chalmers University of Technology, Gothenburg, Sweden. Currently, he is affiliated with the Systems and Control Group of Uppsala University.

Dr. Stoica is a Corresponding Member of the Romanian Academy.